



UNIVERSITÀ
DI SIENA
1240

University of Siena – Department of Medical Biotechnology Doctorate in Genetics,
Oncology and Clinical Medicine (GenOMeC)

XXXV Cycle (2019-2022)

Coordinator: Prof. Francesca Ariani

**Application of the CRISPR-Cas9 genome editing approach for the correction of
the p.Gly2019Ser (c.6055G>A) LRRK2 variant in Parkinson Disease.**

Scientific disciplinary sector: MED/03 – Medical Genetics

Tutor:

Prof.ssa Francesca Ariani

PhD Candidate:

Giada Beligni



**UNIVERSITÀ
DI TRENTO**



**Dipartimento di
Biologia Cellulare, Computazionale e Integrata**

Trento, 24 October 2022

To the Collegio Docenti GenOMeC

Object: Evaluation of Giada Beligni's thesis

I read with interest Giada Beligni's thesis. Her work is clear and well written.

Results are robust and critically discussed. My opinion is that Giada is ready to defend her PhD.

Below, I listed some minor issues Giada should cope with.

Introduction

pag.7 DBS is normally proposed to young patients

pag. 10 the previous name of LRRK2 protein was dardarin, not dandarin

pag.11 LRRK2-PD is not always characterized by LB deposition

pag.11 I don't get the meaning of the sentence "Most of the effects linked to p.G2019S mutation are associated with the GTPase and Kinase activity"

M&M

It is not clear the source of human samples and whether they got an ethical clearance for their use

Results

section 4.3.1 introduces the use of "mutant murine fibroblasts". What does this mean? No tg mice have been included in this study, apparently.

Università degli Studi di Trento

Polo Ferrari 2

via Sommarive, 9 – 38123 Trento (Italy)

P.IVA – C.F. 00 340 520 220

www.unitn.it



**UNIVERSITÀ
DI TRENTO**



**Dipartimento di
Biologia Cellulare, Computazionale e Integrata**

section 4.3.2 introduces “patients fibroblasts”. Did they gather specimen from PD patients carrying the G2019S mutation? Clinical and demographic data are necessary

Fig.19 why the first two controls cell lines do not express LRRK2? Were control and G2019S lines gender and age matched?

Some typos scattered: pag 27 “evidencenced”, pag 29 “Unfortunately,,,”

prof. Giovanni Piccoli

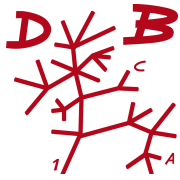
Università degli Studi di Trento

Polo Ferrari 2

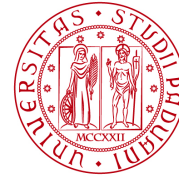
via Sommarive, 9 – 38123 Trento (Italy)

P.IVA – C.F. 00 340 520 220

www.unitn.it



DeBio
DEPARTMENT OF BIOLOGY



UNIVERSITÀ
DEGLI STUDI
DI PADOVA

DEPARTMENT OF BIOLOGY

Dr. Elisa Greggio

Associate Professor of Physiology

Via Ugo Bassi 58/b, 35131 Padova

tel +39 049 8276244

fax +39 049 8276300

[E-mail: elisa.greggio@unipd.it](mailto:elisa.greggio@unipd.it)

Padova, 23 October, 2022

Report for Giada Beligni's PhD thesis

General comments.

The PhD thesis by Giada Beligni explored the possibility of using genome editing approaches based on CRISPR/Cas9 to correct the Parkinson's disease (PD) associated mutation G2019S-LRRK2. The approach is challenging but if successful it would lead to a breakthrough discovery in the field of PD therapeutics.

Overall, the scientific hypothesis, the appropriateness of the experimental approach and the data analysis are of high level and I do not ask to add additional experiments, which I find completely satisfactory for a PhD thesis. However, the structure/flow/style of the manuscript and the accuracy and appropriateness of the references need to be revised as suggested in details below.

Introduction

Correct GBA with GBA1

Gene names need to be in italic

GBA mutations are not recessive, they are heterozygous

VPS13C: add and briefly discuss the latest papers by De Camilli's group on the function of VPS13C as a lipid transfer protein

LRRK2: The N-terminus does not interact with ROC (see Cell paper by Myasnikov 2021). The C-term is NOT involved in dimerization. Please review this part. I also suggest to include a more detailed discussion about LRRK2 physiological function and how mutations affect this function

Page 14: Levedopa is not a dopamine agonist! It is a precursor of dopamine

Material and methods

Please add the animal authorization for mouse work

Results

I have no specific comments here. The approach is challenging and I appreciated that different strategies have been tested and implemented. Did you consider to use viral-mediated expression instead of transfection to increase the efficiency?

Discussion

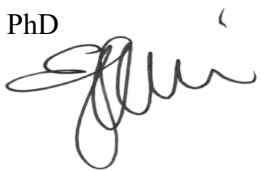
Page 47: “In many people, thinking is impaired, or patients may develop dementia”. Please rephrase, e.g. a subset of patients also display cognitive impairment

Please comment about pros and cons of a gene therapy approach for a disease (G2019S-LRRK2 PD) for which the penetrance is relatively low especially around 60 years of age. Please add discussion as to how this type of strategy could be effectively implemented in the clinics and comment about advantages and disadvantages over LRRK2 kinase inhibitors, presently in phase 11b clinical trials. In general, add a more comprehensive and general discussion about using a gene therapy approach for a disease that is not fully penetrant and late onset

There are typos throughout the text, please revise.

Padova, 23 October, 2022

Elisa Greggio PhD

A handwritten signature in black ink, appearing to read 'Elisa Greggio', is positioned to the right of the typed name. A vertical line is drawn to the right of the signature.

INDEX

- Abstract	3
1. Introduction	4
1.1 Parkinson disease	4
1.2 Genetics of PD and encoded proteins	7
1.2.1 SNCA	8
1.2.2 GBA1	8
1.2.3 PINK1 and PRKN	8
1.2.4 VPS13C	9
1.2.5 The Leucine rich repeat kinase 2 Gene (LRRK2)	10
1.3 The CRISPR/Cas9 system	11
1.4 CRISPR/Cas9 and genome editing	13
1.5 Gene therapy in PD	13
1.6 A new promising tool: the Base Editor system	15
2. Aim of the study	17
3. Materials and methods	18
3.1 Cell line establishment and maintenance	18
3.2 SgRNA and plasmid cloning	19
3.2.1 Mouse model plasmid	19
3.2.2 Human model plasmid	20
3.3 Plasmid extraction	21
3.4 Transfection	21
3.5 Evaluation of red and green fluorescent cells using FACS	22
3.6 Flow cytometry analysis	22

3.7 DNA extraction	22
3.8 Ion Torrent S5 sequencing and NGS analysis	23
3.9 Immunoblot	23
4. Results	25
4.1 Plasmid design	25
4.2 Validation of sgRNA specificity for the mutated allele	26
4.3 Validation of plasmid functionality in primary fibroblasts	28
4.3.1 The mouse model	28
4.3.1.1 A new strategy for the mouse model	30
4.3.1.2 Changing the promoter for the mouse model	34
4.3.2 The human model	36
4.3.2.1 Adenine Base Editor for human PD model	39
4.3.2.2 SpCas9 strategy for G2019S mutation	42
5. Discussion and future perspectives	46
6. Bibliography	51
7. List of the abbreviations	66

ABSTRACT

Parkinson's disease (PD) is one of the most common long-term degenerative disorders that affect the nervous system. Clinical symptoms are bradykinesia, resting tremor and postural imbalance due to the loss of dopaminergic neurons in the substantia nigra pars compacta. Heterozygous mutations in the *Leucine Rich Repeat Kinase 2* gene (*LRRK2*) have been identified both in familial and sporadic cases of PD. The most common variant is the p.Gly2019Ser substitution (c.6055G>A). To date there is no effective treatment available.

The genome editing tool CRISPR/Cas9 has recently transformed the field of biotechnology and biomedical discovery, posing the basis for the development of innovative treatments. Using CRISPR/Cas9 technology and Homology Directed Repair, our project aims to validate gene editing as an alternative therapeutic approach for PD through the genetic correction of the pathogenic p.Gly2019Ser *LRRK2* mutation restoring the wild-type sequence both in human and mouse models. Specifically, we tested various strategies, based on the CRISPR/Cas9-based genome editing technique, for the correction of *LRRK2* p.Gly2019Ser (c.6055G>A) variant in primary mouse and human fibroblasts with promising results. If the correction experiments in *in vitro* models will confirm the good efficiency of the approach, these experiments will represent a fundamental step for the subsequent evaluation of the potential of gene therapy for the treatment of PD as well as other brain disorders for which no therapy is currently available.

1. INTRODUCTION

1.1 Parkinson Disease

Described for the first time by James Parkinson in 1817, Parkinson disease (PD) (OMIM #168600) also known as shaking palsy, is the second most common neurodegenerative disorder worldwide[1], accounting for the 4% of the population beyond 65 years of age; this percentage rises up to 8% with increasing age. Only 5-10% of the patients show a juvenile onset between 21 and 40 years [1].

The disease, influenced by both genetic and environmental factors, is characterized by the loss of dopaminergic neurons in the substantia nigra pars compacta (SNpc) and the presence of intracytoplasmic inclusions called Lewy bodies (LB) mainly composed of α -synuclein and ubiquitin [2,3]. α -synuclein is normally present in synapses where it plays a role in the synaptic vesicle function [4]. An abnormal structure of α -synuclein can result in a misfolded protein, that becomes insoluble and creates amyloid aggregates. These aggregates accumulate and precipitate inside the cells forming intracellular inclusions: the LBs. LBs are involved in the impairment of several important pathways, such as lysosomal and mitochondrial functions, leading to dopaminergic neuronal degeneration (Fig.1) [5]. The ubiquitin-proteasome system, designed to break down the abnormal proteins, also seems to be impaired in this disorder. In fact, α -synuclein clearance is not functioning properly promoting the accumulation of the misfolded and aggregated form [6,7].

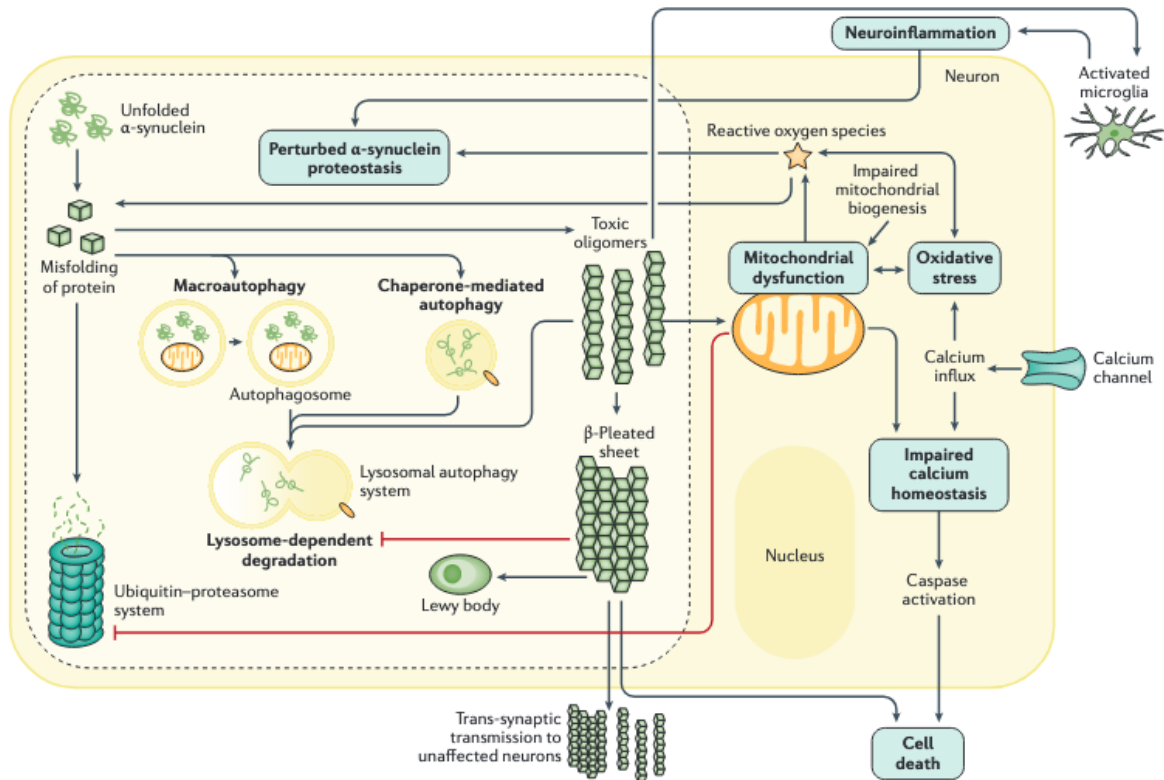


Fig 1: **The molecular mechanism involved in Parkinson Disease.** Schematic view of the major molecular pathways involved in Parkinson disease. Figure taken from *Poewe et al. 2017* [5]

The disease involves structures located in different brain regions, such as the basal ganglia (nucleus caudate, putamen) which are involved in the proper execution of movements [8]. The onset begins silently, in fact it has been proven that, at the time of the diagnosis, more than 60% of dopaminergic neurons have already been lost [9]. In the terminal stage of the disease, LB are found throughout the brain, nerve cord and peripheral neurons [10]. During the progression of the disease, the loss of dopaminergic neurons results in the well known motor features such as tremor, bradykinesia, rigidity and postural instability with changes in posture and gait [11]. There are also non motor symptoms such as hyposmia, memory loss, depression and sleep disturbances [12]. Of the clinical features described above, bradikinesia is the most important character to be identified in order to make a diagnosis of PD.

During the disease progression the Hoen and Yahr scale is used to classify the stage of the disorder [13] (Fig.2). Death comes approximately 10 years after the beginning of the first symptoms and it is related to disease complications.

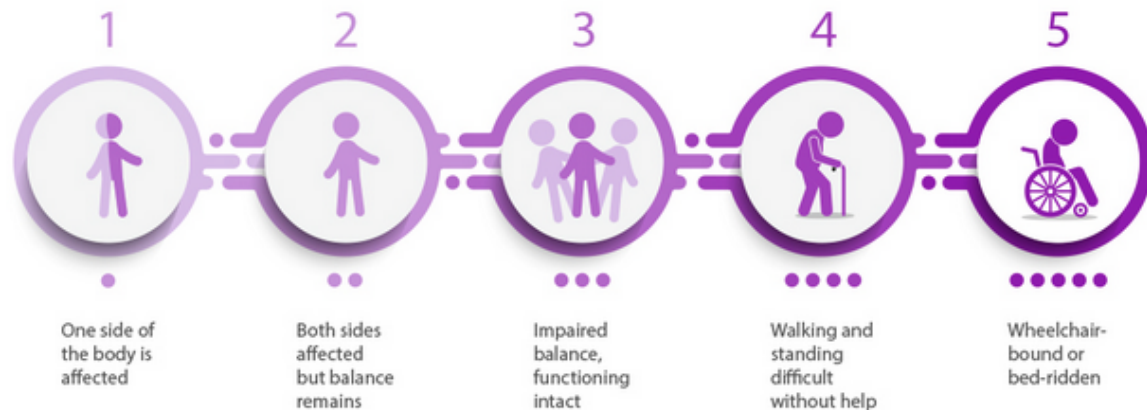


Fig2: The Hoen and Yahr scale for PD progression classification. Explicative image of the stages of the Hoen and Yahr scale which set 5 different stages of injury and disability from unilateral damage, without major symptoms, to stage five, where the patient is not autonomous and confined in a wheelchair. The figure is taken from <https://mobile.hksh.com/en/physio-our-services/neurological-rehabilitation/parkinsons-disease>.

Unfortunately, no definitive therapy is available; the gold standard is the usage of Levodopa, a dopamine precursor, which is able to cross the blood-brain barrier (BBB) and is then converted to dopamine in dopaminergic neurons in the Central Nervous System (CNS) [14]. Levodopa is usually associated with Carbidopa but they are only able to treat the symptoms, not providing a definitive cure for the disease. Alternative approaches such, as Deep Brain Stimulation (DBS) are also proposed as therapy, especially in young patients [15].

1.2 Genetics of PD

Even if the majority of PD cases are sporadic, with unknown etiology, about 15% of the patients present a family history of Parkinson disease [16]. Starting from the discovery of α -synuclein, the first gene associated with PD, other genes have been associated with PD: *parkin* (*PARK2*), *UCH-L1* (*PARK5*), *PINK1* (*PARK6*), *DJ-1* (*PARK7*), *LRRK2* (*PARK8*), and *ATP13A2* (*PARK9*); but there are also *GBA*, *VPS35*, *EIF4G1*, *PARK16* which have been suggested to be responsible for PD based on linkage analysis in familial cases [17]. Among these, 6 genes have been strongly linked to PD (Table 1).

Locus symbol	New designation [†]	Gene locus	Gene	OMIM (phenotype MIM number; gene/locus MIM number)	Clinical clues
Autosomal dominant Parkinson disease					
<i>PARK1</i> or <i>PARK4</i>	PARK-SNCA	4q22.1	SNCA	• 168601; 163890 (<i>PARK1</i>) • 605543; 163890 (<i>PARK4</i>)	Missense mutations (<i>PARK1</i>) cause classic Parkinson disease phenotype. Duplication or triplication of this gene (<i>PARK4</i>) causes early-onset Parkinson disease with prominent dementia
<i>PARK8</i>	PARK-LRRK2	12q12	LRRK2	607060; 609007	Classic Parkinson disease phenotype. Variations in <i>LRRK2</i> include risk-conferring variants and disease-causing mutations
<i>PARK17</i>	PARK-VPS35	16q11.2	VPS35	614203; 601501	Classic Parkinson disease phenotype
Early-onset Parkinson disease (autosomal recessive inheritance)					
<i>PARK2</i>	PARK-Parkin	6q26	<i>PARK2</i> encoding parkin	600116; 602544	Often presents with lower limb dystonia
<i>PARK6</i>	PARK-PINK1	1p36.12	PINK1	605909; 608309	Psychiatric features are common
<i>PARK7</i>	PARK-DJ1	1p36.23	<i>PARK7</i> encoding protein deglycase DJ1	606324; 602533	Early-onset Parkinson disease
<i>PARK19B</i>	PARK-DNAJC6	1p31.3	DNAJC6	615528; 608375	Onset of parkinsonism between the third and fifth decades of life
Complex genetic forms (autosomal recessive inheritance)[‡]					
<i>PARK9</i>	PARK-ATP13A2	1p36.13	ATP13A2	606693; 610513	Early-onset parkinsonism with a complex phenotype (for example, dystonia, supranuclear gaze palsy, pyramidal signs and cognitive dysfunction); also known as Kufor-Rakeb syndrome
<i>PARK14</i>	PARK-PLA2G6	22q13.1	PLA2G6	256600; 603604	PLAN (or NBIA2) is characterized by a complex clinical phenotype, which does not include parkinsonism in the majority of cases
<i>PARK15</i>	PARK-FBXO7	22q12.3	FBXO7	260300; 605648	Early-onset parkinsonism with pyramidal signs and a variable complex phenotype (for example, supranuclear gaze palsy, early postural instability, chorea and dystonia)
<i>PARK19A</i>	PARK-DNAJC6	1p31.3	DNAJC6	615528; 608375	Juvenile-onset parkinsonism that is occasionally associated with mental retardation and seizures
<i>PARK20</i>	PARK-SYNJ1	21q22.11	SYNJ1	615530; 604297	Patients may have seizures, cognitive decline, abnormal eye movements and dystonia
<i>PARK23</i>	Not yet assigned	15q22.2	VPS13C	616840; 608879	Young-adult-onset parkinsonism associated with progressive cognitive impairment that leads to dementia and dysautonomia

Table 1: The main genes associated with Parkinson disease. In red squares the most common genes associated with PD. The table has been modified from *Poewe et al. 2017* [5]

1.2.1 SNCA

The *a-synuclein* (*SNCA*) gene, located on the long arm of chromosome 4 (4q21. 3-22) is the first gene that has been linked to PD, with the first mutation ever identified: c.157c>A (p.A53T) [18]. More studies have identified other dominant mutations (p.A30P, p.E46K, p.H50Q, p.A53E) that definitely prove the linkage with PD [19-23]. Dominant mutations in *SNCA* are typically fully penetrant and linked to fast progressive disorder. These patients show a rapid disease progression with early dementia and Lewy bodies pathology (DLB).

1.2.2 GBA1

The *Glucocerebrosidase* gene (*GBA1*), located on the chromosome 1 (1q21), encodes for a lysosomal enzyme which can degrade the glucocerebrosidase. *GBA1* represents one of the most important known genetic risk factors for PD. Heterozygous *GBA1* mutations are present in between 5 and 25% of PD patients. Mutations in *GBA1* influence the aggregation of α -synuclein and interfere with the lysosomal clearance pathway [24].

1.2.3 PINK1 and PRKN

Mutations in *PTEN-induced kinase 1* (*PINK1*) and *parkin RBR E3 Ubiquitin Protein Ligase* (*PRKN*) genes, located respectively on chromosome 1 and 6, represent the major cause of autosomal recessive (AR) PD. Characterized by an early onset, they account for 77% of juvenile PD cases [25]. Mutations in these genes are linked to mitochondrial dysfunction. In fact, *PINK1* kinase activity is required for the translocation of Parkin to mitochondria and for mitophagy [26,27].

1.2.4 VPS13C

Recessive mutations in *vacuolar protein sorting 13c (VPS13C)* gene (located on chromosome 15) have been reported for the first time in 2016 [28]. All patients show the same phenotype with asymmetric stiffness and a rapid progression with severe and early cognitive dysfunction [29]. Recessive mutations in this gene have been reported to alter mitochondrial functions and PINK1/parkin dependent mitophagy [30]. VPS13C has also been reported to be involved in lipid exchange between organelles; specifically, it is bound to the endoplasmic reticulum (ER) and tether lipids to late endosomes and lysosomes. The absence of VPS13C has been associated to lysosomal dysfunction in protein degradation and to an altered lipid profile [31,32].

1.2.5 The Leucine rich repeat kinase 2 gene (LRRK2)

The *Leucine rich repeat kinase 2* gene (*LRRK2*) is located on the long arm of chromosome 12, in 12q12, and encodes for an unusually large protein (2527 amino acids) known as *Dardarin* (Fig.3a).

LRRK2 is a kinase protein composed by different domains (Fig. 3b): a Ras of Complex G-domain (Roc) and a Carboxy terminal of ROC domain (COR)[33]; at the N and C termini of the protein there are protein-protein interaction domains: a conserved N-terminal armadillo (ARM) domain, and a C-terminal WD40 domain [34,35].

The architecture of the gene and the presence of multiple protein-protein interaction regions (Fig.3b) suggests that LRRK2 may function as a scaffold protein, making an essential contribution to the formation of a multiprotein signaling complex [36].

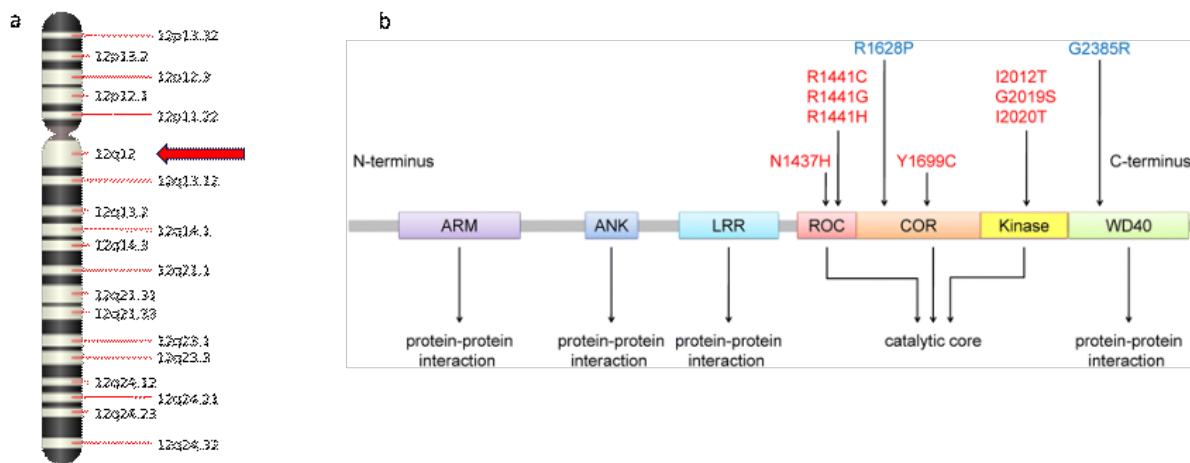


Fig 3: Location LRRK2 gene and protein domain composition. The LRRK2 gene is located on the long arm of the chromosome 12 (a, red arrow). The protein encoded by this gene is composed of several domains (b). the picture also shows the mutations identified in the different domains. The mutations in red are the one classified as pathogenic while the light blue ones are classified as uncertain (clinVar).

LRRK2 is widely expressed throughout the body, especially in the kidney, lungs and brain, and in particular in the putamen, target place of the neurons of the substantia nigra [37]; it is also widely expressed in immune cells, such as B cells, microglia, macrophages and monocytes [38-40] and its expression is tightly regulated by immune stimulation. Moreover, LRRK2 has been biochemically associated with inflammatory and autophagoc pathways [41]. In addition, polymorphisms in LRRK2 have been reported to be associated with inflammatory diseases, such as Inflammatory Bowel Disease (IBD) or an increased susceptibility to leprosy [42,43]. Dominant mutations in the *LRRK2* gene (Fig. 3b) have a variable penetrance and patients show a late onset disease with dementia and early LB formations with α -synuclein-positive pathology.[44]. To date, only six of the 20 mutations identified in this gene have been proven to be pathogenic (Fig. 3b) [45]. The most common variant is the hotspot c.6055G>A (p.(Gly2019Ser)), located in the kinase domain of the protein, accounting for 4% of familial and 1% of sporadic cases of PD [46]. Patients carrying this mutation are more susceptible to develop Lewy body pathology [47]. Moreover, a recent study has shown that p.G2019S patients present a typical levodopa responsive parkinsonism with tremor as an early feature

[48]. p.G2019S mutation results in a gain of function with an increased kinase activity [49-51], leading to a reduced mitophagy in dopaminergic neurons and microglia [52]. LRRK2 kinase hyper-activation leads also to an impairment of the late stages of endocytosis and lysosomal traffick [53-55]. Moreover, it has been linked also to an alteration of autophagosome axonal transport [56].

1.3 The CRISPR/Cas9 system

CRISPR is an adaptive bacterial immune system directed against viruses. It was first described in 1987 in *E.coli* genome as a locus containing repeated sequences with an unknown function [57]. In 2005, following the discovery of the Protospacers Adjustment Motif (PAM), *Pourcel et al* reported that CRISPR elements acquire new repeats from bacteriophage DNA [58,59]. In 2007, *Barrangou et al.* demonstrated the association with the CRISPR-associated (Cas) gene and how they are used as an adaptive immunity which can provide resistance against bacteriophage infection [60].

The CRISPR/Cas9 adaptive immune system acts in three steps (Fig.4):

- acquisition of CRISPR, where the invading nucleic acid is processed in small DNA fragments, called protospacers, which are then incorporated in the CRISPR Locus of the bacterial genome; each locus is separated by repeated sequences named Protospacers adjacent motifs (PAM) strictly associated with the type of Cas9 involved in the process [61].

- *crRNA biogenesis*, where the entire CRISPR locus is transcribed in a long precursor, named the pre-crRNA, which is then cleaved by an endogenous RNase III. The cutting generates a mature crRNA consisting of one spacer and a repeated motif [62].
- *interference with invading DNA*, where the mature crRNA guide the Cas9 protein to the adverse nucleic acids to cleave and degrade them [63].

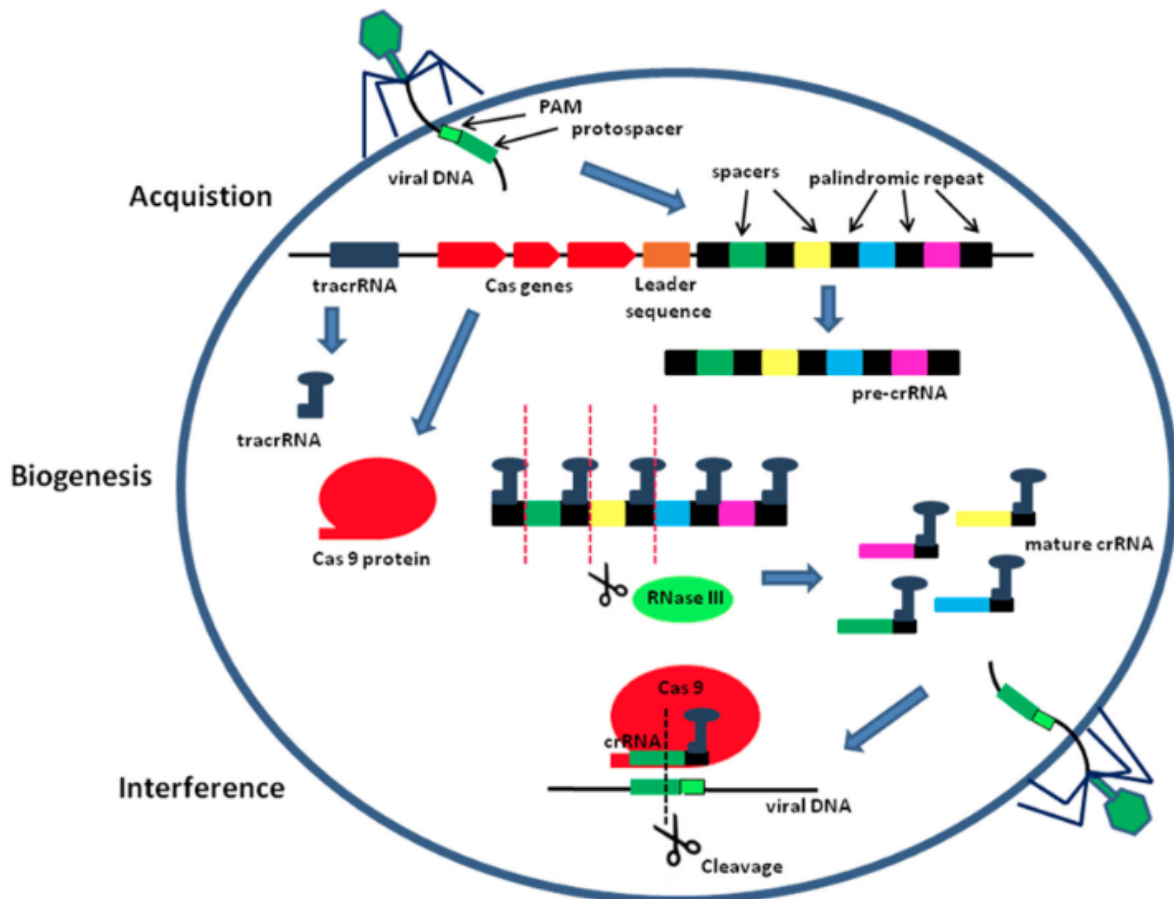


Fig 4: The biogenesis and activation of CRISPR-Cas9 in bacteria. When a viral infection is coming out, the viral nucleic acid is cutted into small pieces and inserted inside the CRISPR locus in between a palindromic repeated sequence named PAM. The entire CRISPR locus is then transcribed giving rise to a pre-crRNA, which is then processed by the RNaseIII (in green) and cleaved into small pieces of mature crRNA. At this point, the mature crRNA is able to guide the Cas9 protein to the viral DNA in order to cleave and degrade it. Picture taken from Hryhorowicz, M. et al. 2017. [65]

1.4 CRISPR-Cas9 and genome editing

In 2012 CRISPR became a revolutionary tool that researchers used in laboratories all over the world becoming a widely used system also for genome editing [66]. Indeed, CRISPR can be efficiently reprogrammed to be able to recognize a specific DNA sequence inside the cell's DNA. This is possible by the generation of a single guide RNA (sgRNA) which is able to recruit the Cas9 nuclease and to guide it to a specific genomic location by a Watson-Crick base pairing [67]. A double strand DNA break (DSB) follows the pairing of the guide to its target sequence. The break can be repaired by nonhomologous end joining (NHEJ), which is an error-prone process able to lead to the creation of insertions and deletions. In the presence of a donor sequence Homology-Directed Repair (HDR) can be exploited to precisely modify single nucleotides, for example to correct pathogenic mutations [68]. CRISPR/Cas9 editing coupled to HDR is currently being largely studied for therapeutic genome editing. In fact, recent studies show that it can be applicable to many disorders, including sickle cell anemia, β -thalassemia, muscular dystrophy and Rett Syndrome [69-72].

1.5 Gene therapy and Parkinson disease

The current gold standard for PD treatment is represented by Levodopa, a dopamine precursor, or Deep Brain Stimulation (DBS) which is usually proposed in young PD patients [73]. Unfortunately, these treatments don't represent a definitive cure for PD, since they are only able to slow down the progression of the disease. Moreover, during disease progression, the efficacy of the pharmacological treatment is reduced, despite the increasing dosage of the drugs.

Gene therapy approach was first described in 1972 [74]. From that date, we assisted to an extremely fast evolution in this field bringing us fastly to use gene therapy to treat diseases.

From the early 2000s there has been an increase in the number of gene therapy clinical trials all over the world and the first drugs start to be approved [75]. After 2015, the Food and drug administration (FDA) approved different drugs like Strimvelis™ for Adenosine Deaminase deficiency (ADA-SCID), [76] or Spinraza™ and Exondys 51™ for the treatment of Spinal Muscular Atrophy (SMA) and Duchenne Muscular Dystrophy (DMD), respectively [77,78].

The first publications regarding a possible approach of gene therapy for neurodegenerative disorders, and in particular for Parkinson disease, came out in the early 2000s. The first attempt of gene therapy tried to use cells and tissue transplantation in order to increase the dopamine content [79-81]. In 2002, Muramatsu et al demonstrated how the intraputaminial gene delivery of dopamine-synthesizing enzymes, such as the Aromatic L-Amino Acid Decarboxylase (AADC), could result in transgene expression and restoration of putaminial dopaminergic levels [82]. Subsequently, viral vector technology was established as a new method for the efficient delivery of genetic material to the target place [83]. The usage of Lentiviral vectors has even reached the clinical trials for enzyme replacement in PD [84].

Recently, gene editing tools such as CRISPR (clustered regularly interspaced short palindromic repeats) -Cas9 (CRISPR associated enzyme) have sparked a significant interest in this field. CRISPR-Cas9 appears in fact to be one of the most promising gene-editing techniques available. The success of using CRISPR-Cas comes from its easy use, efficacy and capacity to edit several genes. This revolutionary technology thus seems to be a promising approach in PD gene therapy [85,86].

1.6 A new promising tool: The Base editor system

In 2016 *Komor et al* published their work where they described their new tool: the “cytidine base editor” (CBE). CBE is able to induce the direct conversion of a C to a T or of a G to an A at a programmable target locus using a naturally occurring deaminase enzyme, able to convert a target cytosine to uracil (fig 5a). Neither DSB nor Donor DNA are needed in this process [87]. The next year *David Liu et al.* published a work describing another base editor: the Adenine Base Editor (ABE) which is able to efficiently convert an A to G or a T to C [88]. The ABE works with a modified deoxyadenosine deaminase (TadA) and an nCas9, a catalytically impaired Cas9 which is not able to make DSB (fig.5b). The CBE works in the same mode but using the Cytidine deaminase enzyme.

The ABE system is basically guided by an sgRNA to a target site where the TadA can convert the adenine (A) to inosine (I) which is replicated by the polymerase as a Guanine (G) [89].

In the subsequent period, BE capacities have been further exploited with the development of further generation of BE systems. [90] In fact, seven different generations of base editors have been developed till now, applicable in both human and animal models [91,92].

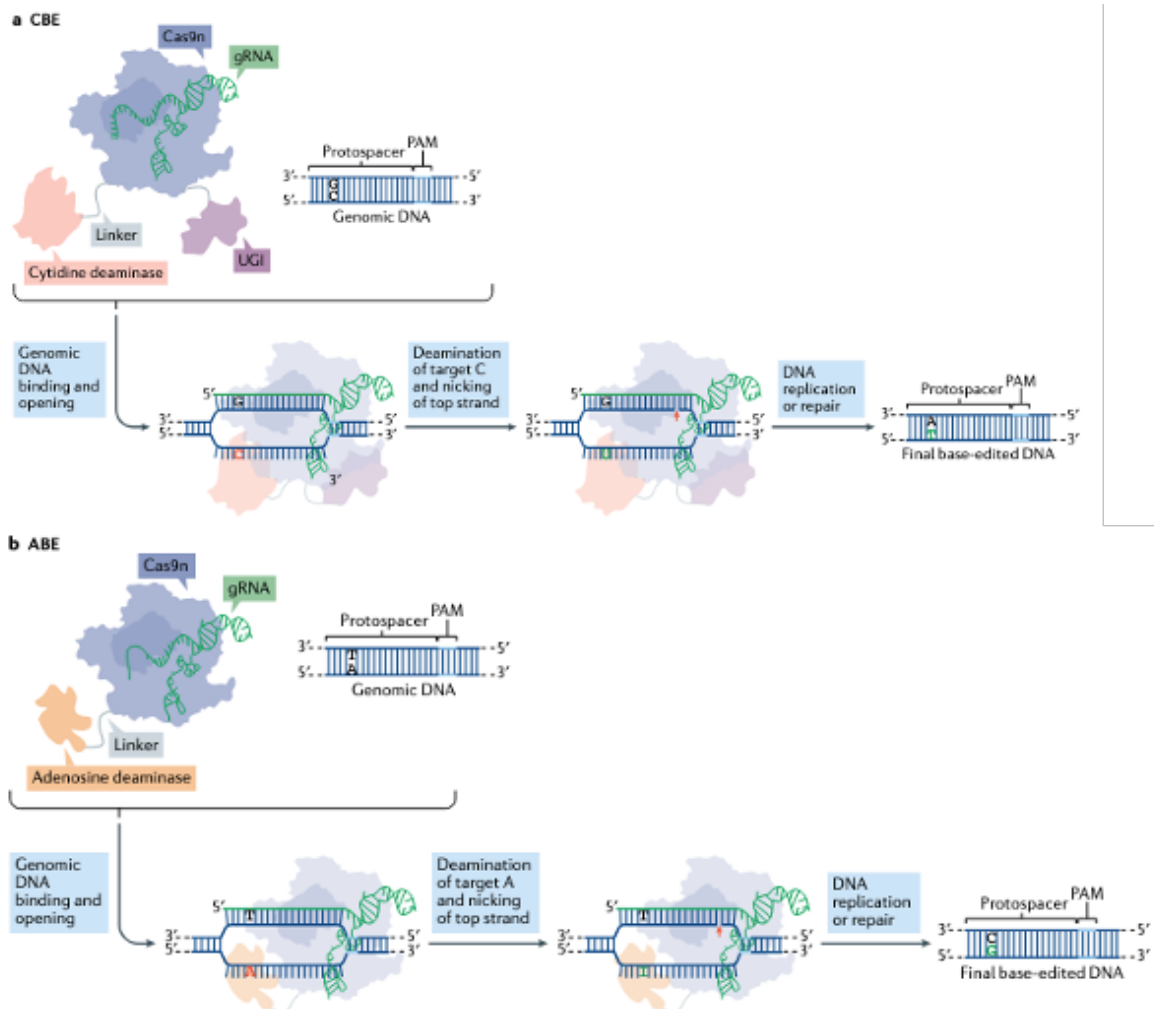


Fig 5: Overview of the base editor technology Representative image of the working flow of the Cytosine base editor (a) and the Adenine Base editor (b) systems. The figure is modified from Zhang, X.,*et al. Nat Biotechnol* 38, 856–860 (2020) [93].

Recently the applicability of the base editor systems started to be investigated also in gene therapy; for example ABEs have been used to efficiently rescue sickle cell disease in animal models and in Hutchinson-Gilford progeria syndrome (HGPS) patients [94,95]. On the other side, CBE has been investigated in Fanconi Anemia [96]. In conclusion, our knowledge of the potentiality of BE is still partial, but it seems to represent a very promising tool for the future of gene therapy.

2. AIM OF THE STUDY

Parkinson disease (PD) is the second most common neurodegenerative disorder worldwide characterized by clinical motor symptoms such as bradykinesia, resting tremor and rigidity. PD it has been associated with both genetic and environmental factors. During the last few years, several genes have been associated with PD and one of the most commonly altered is the *LRRK2* gene.

The overall goal of this study is to develop a CRISPR/Cas9-based approach in order to target the c.6055G>A p.Gly2019Ser recurrent mutation in *LRRK2* gene and to validate the system in both mouse and patient-specific cell models. Particularly we focused on:

- Design of a CRISPR/Cas9 - based tool for mutation correction by gene editing .
- Validate the designed strategy in mouse and patient derived cell models.

The results of this work will set a starting point for future studies for the development of a new gene therapy for Parkinson disease, representing a hope for the treatment of this disorder.

3. MATERIALS AND METHODS

3.1 Cell line establishment and maintenance

Mouse primary fibroblasts were obtained from sacrificed animal's ears and tail (gently provided by Prof. M. Morari, University of Ferrara). Mouse ears were incubated in 70% ethanol for 5 minutes, then cutted in small pieces (size 3-4 mm) and incubated in enzymatic mix (0,01g pronase, 5uL TRIS buffer pH8.0; water til volume) at 37° for 90 minutes. The obtained digestion is then crushed with the plunger of a syringe, transfered in a 15mL falcon tube and centrifuged for 7 minutes at 580XG at 4 ° C. The pellet is resuspended in 10mL of complete medium (FBS 10%, 500uL L-Glut, 500uL pen/strep, RPMI 1640 to volume). The resuspension is then plated in a 10cm dish and placed in an incubator at 37° with 5% CO₂. The next day fibroblasts are attached on the bottom of the dish. Once cells reach confluence they are passed 1:2 with Trypsin/EDTA (0.05%) solution (Irvine Scientific Santa Ana, California, US). From this point, Chang amnio medium (Irvine Scientific Santa Ana, California, US). completed with 1% of pen/strep, is used.

Three different human primary fibroblast lines harbouring the p.G2019S mutation in *LRRK2* gene were used in this work. Two of them came from the “Cell Line and DNA Biobank from Patients Affected by Genetic Diseases”, member of the Telethon Network of Genetic Biobanks (<http://biobanknetwork.telethon.it>; project no. GTB18001). The third one was obtained from a patient referred to the Medical Genetics Uniti (Azienda Ospedaliera Universitaria Senese) for genetic counseling. Primary fibroblasts were obtained from skin punch biopsy following informed consent signature. Human Fibroblasts were cultured in Chang Amnio Medium and

1% of antibiotics, according to the standard protocol, and routinely passed 1:2 with Trypsin/EDTA (0.05%) solution (Irvine Scientific Santa Ana, California, US).

3.2 sgRNA and plasmids cloning

We designed several systems both for mouse and human models. The system can be either based on two plasmids to be used in combination with a plasmid carrying the Cas9 coding sequence and another containing the sgRNA, under the control of the U6 promoter, the donor DNA which is used for HDR and an mCherry/EGFP system to detect the Cas9 activity; alternatively we also designed an all in one plasmid carrying the Cas9 coding sequence, the sgRNA, the Donor and an EGFP system to detect the entrance of the plasmid inside the cell. The variant-specific sgRNA was designed using the MIT CRISPR Design Tool (<http://crispr.mit.edu>).

3.2.1 Mouse model plasmids

The oligonucleotides used for the cloning are listed in table 2 .

A wild type Donor DNA (#1) was designed as 108bp centered on the mutated nucleotides, where a Protospacer Adjacent motif (PAM) has been identified. The variant specific sgRNA was obtained by annealing and subsequent phosphorylation of single-strand oligonucleotides (#2; #3). The px330 Addgene plasmid encoding *Streptococcus pyogenes* Cas9 (SpCas9) was used for Cas9 cloning.

	Sequence feature	Sequence
# 1	Donor WT	tcgaTTTTTACCCTGTATCCCAATGCTGCCATCATTGCGAAGATTGCGGACTACGG GATCGCACAGTACTGCTGCAGGATGGGAATAAAGACATCAGAGGGCACctag
# 2	SgRNA	CGGGATCGCACAGTACTGCTGCAG
# 3	SgRNA + PAM	
# 4	EF1a promoter	gggcagagcgcacatcgcccacagtccccgagaagtggggggaggggtcggcaattgatccggtgcc tagagaagggtggcgcggggtaaactgggaaagtgatgctgtactggctccgctttttcccagggtg ggggagaaccgtataaagtgcagtagtcgccgtgaacgttcttttcgcaacgggtttgccccagaac acag

Table 2 : Oligonucleotides used for mouse specific plasmid construction

3.2.2 Human model plasmids

The oligonucleotide used for the cloning are listed in table 3.

Targeting construct and the genetic loads were inserted between the two Inverted Terminal Repeats (ITR). A wild type Donor DNA (#1) was designed as 121bp centered on the mutated nucleotide, where a Protospacer Adjacent motif (PAM) has been identified. The variant specific sgRNAs were obtained by annealing and subsequent phosphorylation of single-strand oligonucleotides (#2; #3; #4; #5). For Cas9 plasmid, the PX551 plasmid encoding SpCas9 under the control of the *MECP2* promoter [97] was used as the backbone for the cloning of the XCas9.

For Adenine Base editor strategy the Addgene #108382 plasmid was used to carry the dXCas9.

For this strategy an EGFP fluorescent reporter was inserted outside the ITR.

	Sequence Feature	Sequence
# 1	Donor	TATACCGAGACCTGAAACCCACAATGTGCTGCTTTTCACACTGTATCCCAATGCTGCCATCATT GCAAAGATTGCTGAtTACgGCATTGCTCAGTACTGCTGTAGAATGGGGATAAAAAAC
# 2	sgRNA (xCas9)	GCAGTACTGAGCAATGCTGT
# 3	sgRNA1 (SpCas9)	tGTAGTCAGCAATCTTTGCAATG
# 4	sgRNA2 (SpCas9)	aGCATTGCTCAGTACTGCTGTAGAA
# 5	ABE SgRNA	GCAGTACTGAGCAATGCTGT

Table 3: Oligonucleotides used for human specific plasmid construction

3.3 Plasmid extraction

Plasmids were transformed in STBL3 Competent *Escherichia coli* cells and grown in standard Luria-Bentani (LB) medium [98]. Plasmids were purified with the Plasmid DNA purification (Nucleobond Xtra Midi/Maxi) kit (Macherey-Nagel, Duren, Germany). All constructs were verified using Sanger sequencing using the Big dye Terminator Cycle Sequencing Kit on the ABI Prism 3130 Genetic analyzer sequencer (Applied Biosystem, Foster City, USA). The data have been analyzed with the Sequencer 4.9 software.

3.4 Transfection

HEK293 cells were seeded at a density of 5×10^4 cells/well the day prior to transfection, in order to obtain cells at 70-90% confluency on the day of transfection. Transfection were performed using Lipofectamine™ 2000 Transfection Reagent (ThermoFisher Scientific) according to the manufacturer's protocol. Cells were transfected with 100 ng of targeting plasmid and 400 ng of Cas9 encoding plasmid. Cells were left at 37° for 6 hours, after that time, the medium containing the Lipofectamine reaction reagents medium was replaced with a new one (DMEM with 20% of FBS, supplemented with L-Glutamine).

Fibroblasts, once they have reached the 80-90% of confluences, were harvested with Trypsin Solution and counted using the Burker chamber, 1×10^6 cells were needed for each sample. Cells were transfected with 9ug of total DNA in a 1:3 ratio (1ug of Reporter and 3ug of Cas9). Fibroblasts were transfected using the Neon Transfection System with 10ul and 100ul tips (ThermoFisher Scientific) according to the manufacturer's protocol. The following parameters: 1700V 20" 1P were set on the Neon™ instrument according to the manufacturer's protocol. For each experiment, cells transfected with an empty vector and cells transfected with GFP encoding plasmids were used respectively as a negative and positive control to monitor the transfection efficacy.

3.5 Evaluation of Red and Green fluorescent cells using FACS

The transfection efficiency was assessed starting 24 hours post-transfection by fluorescence microscopy. 48 hours after treatment, cells were detached with Trypsin EDTA 1%. Washed twice with 1mL of Phosphate buffered saline (PBS). EGFP and mCherry positive cells were subsequently quantified with a Cytoflex flow (Beckman Coulter) cytometer with blue (488nm) and a yellow (560nm) lasers, using a 530/30 (EGFP) and a 585/42 (mCherry) filter. For each experiment, non-transfected cells and cells transfected with an EGFP-encoding plasmid were used as negative and positive controls, respectively, to monitor transfection efficiency.

3.6 Flow cytometry analysis and cell sorting

Cells were analyzed and sorted on a fluorescent-activated cell sorter FACS Aria II (Becton Dickinson) using FACS Diva software version 8.0.1 (BD Biosciences-US). To isolate EGFP-positive cells for subsequent analyses, fibroblasts were detached, resuspended in PBS/EDTA 3mM/Trypsin 2.5% (Gibco) and placed on ice. The cellular suspension was filtered through a 70 µm filcon filter (BD Biosciences). Fibroblasts were sorted using a 100 µm nozzle and an event rate of 1000/sec.

3.7 DNA extraction

Total DNA was extracted from sorted cells using using QIAMP DNs Micro Kit (QIAGEN[®], Hilden, Germany) according to the manufacturer's protocol. The DNA concentration was assessed by Qubit[™] 3.0 fluorometer (Thermofisher) according to the manufacturer's protocol.

3.8 Ion Torrent S5 sequencing and NGS analysis

The Ion AmpliSeq 2.0™ Library Kit (Life Technologies™, Carlsbad, CA) was used for library preparation. Libraries were purified using Agencourt AMPure XP system and quantified using the Qubit^R dsDNA HS Assay Kit reagent (Invitrogen Corporation, Life Technologies), pooled at an equimolar ratio, annealed to carrier spheres (Ion spheres Particles, Life Technologies) and clonally amplified by emulsion PCR (emPCR) using the Ion Chef system™ (Ion Chef, Life Technologies). ION 510™; 520™; or 530™ chip were loaded with the spheres carrying single stranded DNA templates and sequenced on the Ion Torrent S5 instrument (Life Technologies™, Carlsbad, CA) using the Ion S5™ Sequencing kit, according to the manufacturer's protocol. For each sample, the FASTQ files of transfected cells and relative controls were downloaded from the sequencing platform (S5 Torrent Server VM) and uploaded to the online analysis tool Cas-Analyzer [99] together with the sgRNA and the Donor in order to obtain the percentage of HDR achieved. For the samples treated with the Adenine Base editor method FASTQ files of transfected cells and relative controls were uploaded to the online tool BE analyzer [100] a JavaScript-based instant assessment tool for NGS data of CRISPR base edited cells.

3.9 Immunoblot

Proteins both from patient-derived and mouse derived fibroblasts and neuronal precursors were extracted with RIPA buffer (Tris-HCl 50 mM, NP-40 1%, Na-Deoxycholate 0.5%, SDS 0.1%, NaCl 150 mM, EDTA 2mM, pH 7.4). Protease inhibitor cocktail (Sigma, Milano, Italy) was added to all lysates. Lysates were cleared by centrifuge at 20.000 g for 30 min at 4 °C. Protein concentration was assessed with the quantum protein assay kit (Euroclone) combining 980 ul of A reagent with 20ul of the B reagent. 2ul of cell lysate was added to the solution. Protein concentration was assessed with Epoch™ microplate spectrophotometer (Agilent). 30 ug of

protein were loaded on Blot Bis Tris Plus precast gel 4-12% (Thermofisher scientific TM) in buffer MES (Invitrogen) and runned at 150 V for 30-40 min. Proteins are transferred on nitrocellulose membrane using the iBlot™ 2 gel transfer device according to the manufacturer's protocol. The membrane was then stained with Ponceau Red (Sigma Aldrich) in order to assess the correct protein transfer.

The membrane was then washed twice with PBS + Tween at 0.002 % for 10 minutes. The membrane is then saturated with PBS-T 0.002% with 5% milk for 1 h at RT, washed twice in PBS-T for 10 minutes. The membrane was then incubated overnight at 4°C with the following primary antibodies: : anti β -Actin (Santa Cruz, Biotechnology, Inc #sc-47778); anti EGFP (Abcam ab184601); anti LRRK2 (Abcam ab133518); anti SaCas9 (Thermofisher Scientific Ref. 61787).

After two washes in PBS-T 0,002%, the membrane is incubated with a horse-radish peroxidase (HRP)-conjugated secondary antibody (mouse or rabbit according to the primary antibody production site) with a 1:1000 dilution. The chemiluminescent signal is then developed with the enhanced chemiluminescence method (Chemidoc™).

4. RESULTS

4.1 Plasmid design

In order to validate the CRISPR/Cas9 application for the correction of the LRRK2 c.6055G>A (p.(Gly2019Ser)) variant we have designed a single guide RNA (sgRNAs) able to target the mutated allele and an appropriate DNA Donor carrying the WT sequence.

We designed a strategy based on two plasmids to be used in combination: the first plasmid expressing the Cas9, under the control of a CMV promoter, and the second one harboring the sgRNA and the DNA Donor together with a dual fluorescent mCherry-eGFP system (Fig.6).

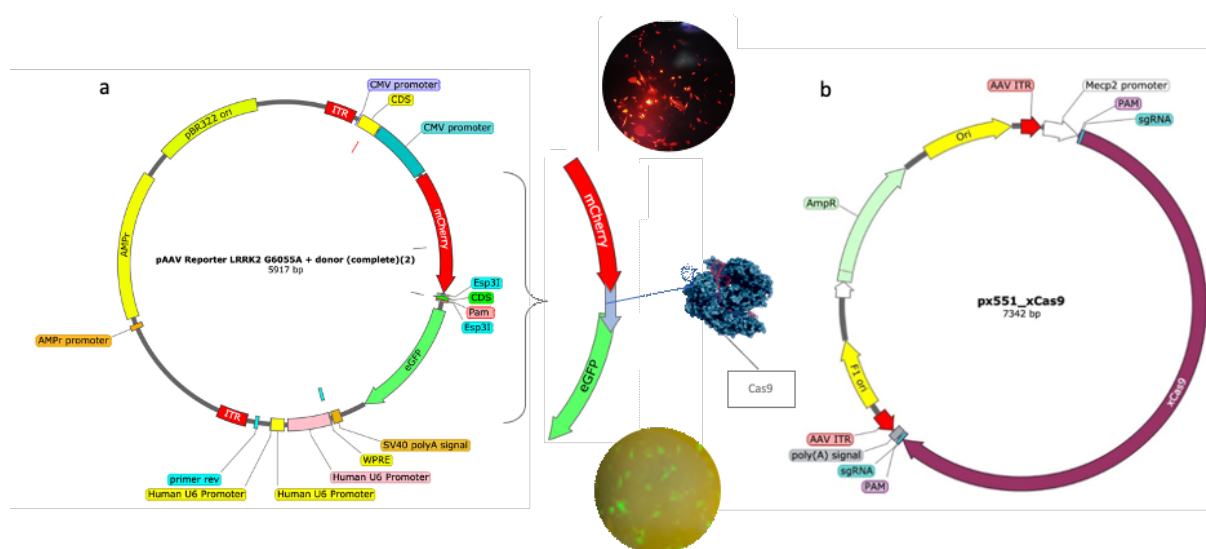


Fig.6: Plasmid design and strategy. Representation of the plasmids and of the selection strategy. a) The reporter plasmid with the sgRNA, the Donor DNA and the mCherry/eGFP fluorescent system under the CMV promoter. b) the Cas9 plasmid with the Cas9 coding sequence, flanked by an sgRNA + PAM for autocleaving. In the middle, an enlargement of the fluorescent reporter system.

The fluorescence system is designed to visualize and monitor the cells post transfection. It is composed by mCherry, which is constitutively expressed, and an eGFP gene which requires the expression and the activation of the Cas9 to be activated. Indeed, a target sequence was inserted between the two fluorescent markers (Fig.6, central panel). Once expressed, Cas9 is

able to recognize and target the sequence between mCherry and eGFP bringing this latter back in frame and resulting in the expression of both red and green fluorescence. A variant-specific gRNA has been cloned on both sides of the Cas9 CDS in order to induce autocleaving and avoid prolonged expression.

4.2 Validation of sgRNA specificity for the mutated allele.

In order to test the functionality of our system, we selected two different sgRNAs that exclusively target the mutated locus: one for the human model where an adjacent XCas9 PAM (NG) was identified, and a second one for the mouse model, where, in order to obtain the same amino acid substitution, a di-nucleotides have been mutated (GGG→TCG). Here an adjacent SpCas9 PAM sequence (NGG) was present [101].

We transfected human embryonic kidney 293 cells (HEK293) with mutation-specific plasmids designed for human and mouse models. Specifically, HEK293 were transfected either with the dual plasmid system where the target sequence in between mCherry/EGFP encoding for wt and mutated sgRNA. If the wt sgRNA is present, no green cells were detected (fig.7a;b) on the contrary, when the mutated sgRNA is present, the activation of the EGFP is evidenced (fig.7a,b), confirming the specificity of the variant specific sgRNAs.

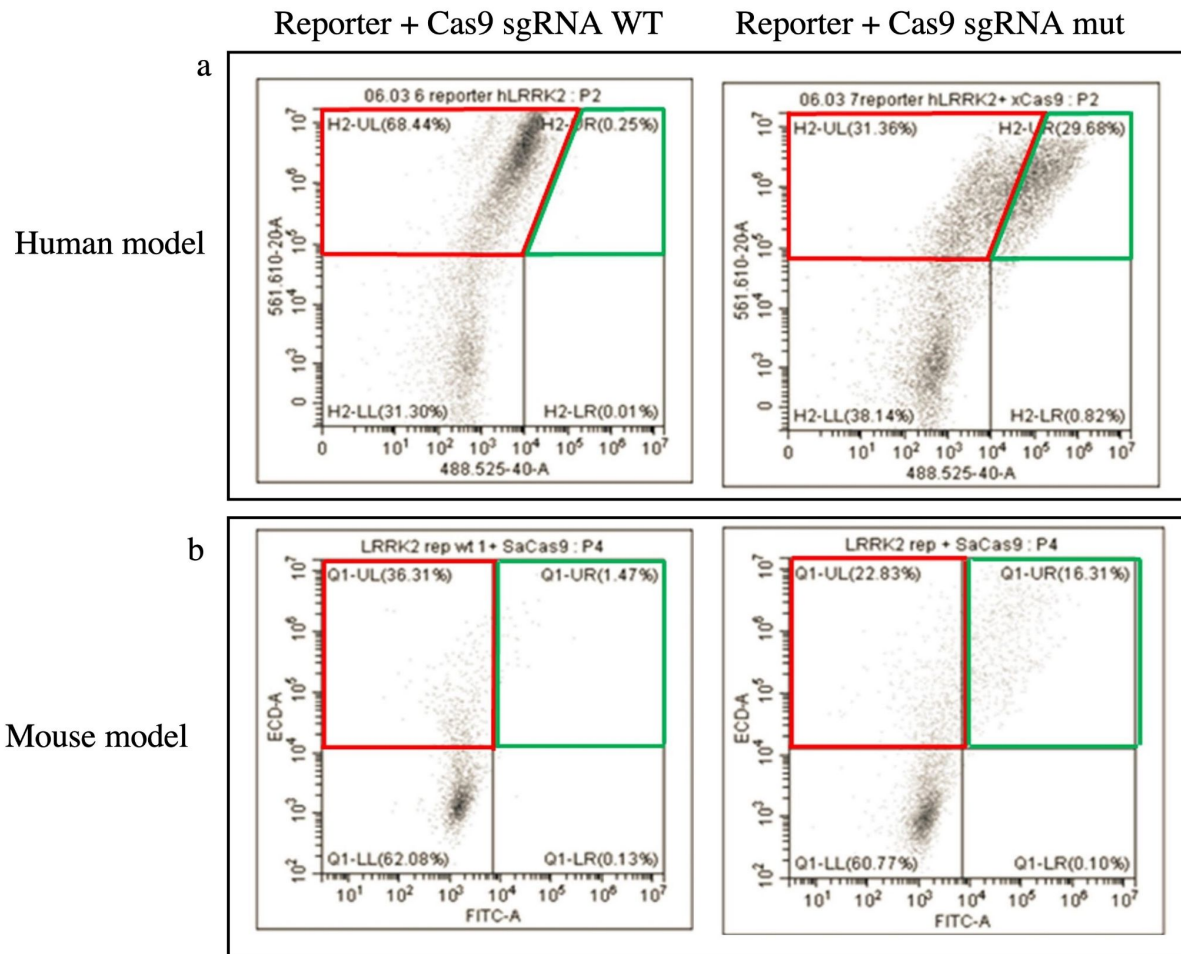


Fig.7: Validation of sgRNA specificity in HEK293. FACS analysis of HEK293 cells transfected with the mCherry/EGFP reporter and Cas9 plasmids a) sgRNA specificity in the human model. On the left is reported transfection results with the WT sgRNA resulting in 68.44% of red cells; on the right is reported the transfection with the mutated sgRNA resulting in 31.36% of red cells, of which, 29.68% are also green. b) sgRNA specificity in the mouse model. On the left is reported transfection results with the WT sgRNA resulting in 36.31% of red cells; on the right is reported the transfection with the mutated sgRNA resulting in 22.83% of red cells, of which 16.31% are also green.

In figure 7a transfection results with plasmids specific for human cells are shown. Transfection with the WT sgRNA resulted in 68.44% of red cells and no EGFP + cells (Fig.7a left); on the contrary, the transfection with the mutated sgRNA (Fig.7a right) resulted in 31.36% of mCherry positive cells, of which 29.68% are also EGFP+.

For the mouse model (Fig 7b), transfection with the WT sgRNA resulted in 36.31% of mCherry positive cells. On the contrary, cells transfected with the mutated sgRNA resulted in 22.83% of mCherry positive cells, of which 16.31% are also EGFP+.

Taken in their entirety, these results confirm the specificity of the variant-specific sgRNAs.

4.3 Validation of plasmid functionality in primary fibroblasts.

4.3.1 The mouse model

In order to assess the functionality of our plasmid design in mutated cells we have made a preliminary transfection test with both reporter and Cas9 plasmid in mouse primary fibroblasts, isolated from tail and ears (gently provided by prof. M. Morari Lab, University of Ferrara) (fig.8). The experimental conditions included a negative control (fig.8a) transfected with an empty plasmid, a positive control (fig.8b) transfected with an EGFP plasmid (gently provided from TIGEM lab in Pozzuoli), and a sample treated with both Reporter and Cas9 plasmids specific for our mutation (fig.8c). 48h post transfection, the EGFP expression was assessed by FACS analysis.

No green cells were found in the negative control (fig.8a lower part), 72.9% of green cells were present in the EGFP transfected cells (fig.8b lower panel) and 17% of green cells (fig.8c lower panel) was obtained in the sample treated with the designed plasmid.

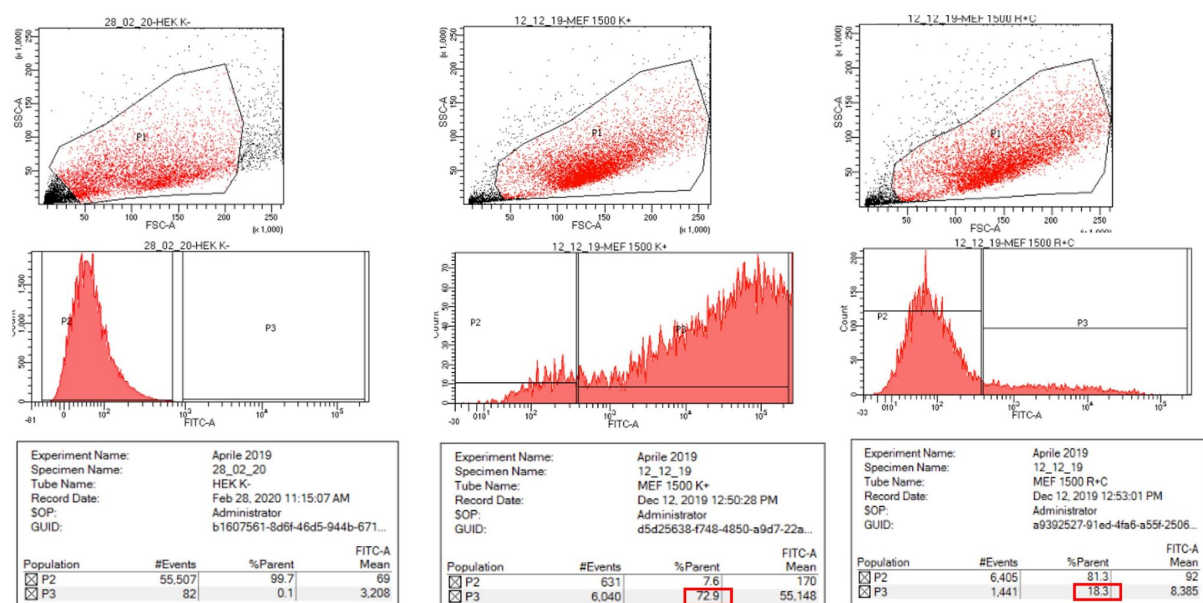


Fig.8:Plasmid functionality validation. Preliminary transfection test results in mouse primary fibroblasts. a) results for the cells transfected with an empty plasmid as negative control; b) cells transfected with the EGFP

plasmid as positive control . Result evidence 72.9% EGFP + cells ; c) transfection with the correction plasmid is shown indicating 18.3% of EGFP + cells.

In order to assess the editing capacity of our system, we performed a new transfection experiment with both the Cas9 and the reporter plasmids in mutated mouse fibroblasts. mCherry positive cells were already visible 24 hours post transfection. EGFP+ cells were recovered 48hours post transfection using FACS. Only 0.1% of green cells were recovered in two independent experiments (fig.9).

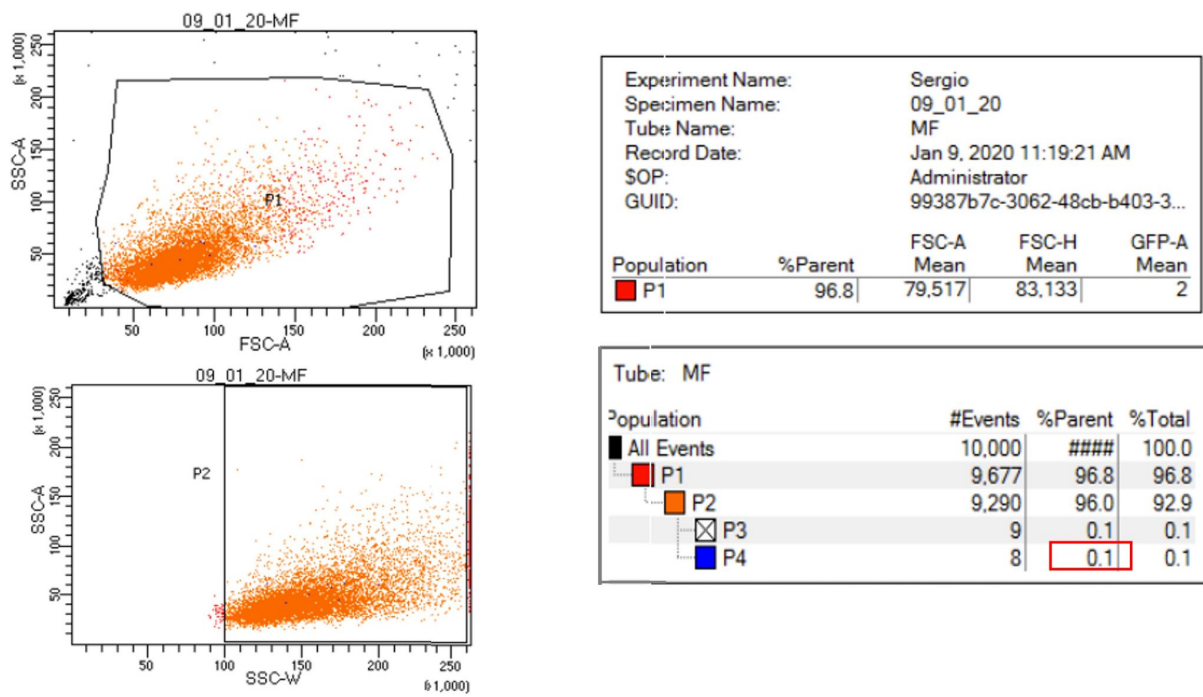


Fig.9: Cell sorting report. FACS sorter report is shown resulting in 0.1% of EGFP+ recovered cells (red square).

Taking into account the previous results, we decided to repeat the preliminary transfection experiment (fig.9) to verify again the functionality of the plasmids. In order to do this, we did a new transfection. 48h post transfection the green fluorescence was assessed via FACS. The results showed a much lower activation of the system, in fact we obtained 3.19% of red cells (fig.10) of which, 4.39% were also green (fig 10).

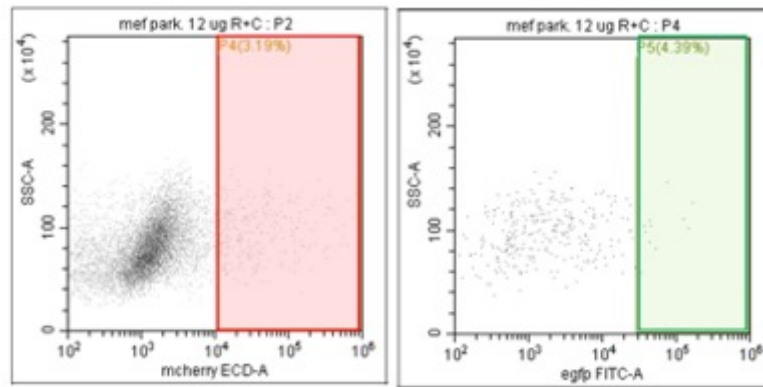


Fig.10: FACS analysis on transfected primary fibroblasts. The graph shows the FACS analysis on transfected mouse primary fibroblasts. On the left, the red fluorescence is evidenced (red box) with a 3.19% of red cells, of which, only the 4,39% are also green (right in the green box).

4.3.1.1 A new strategy for the mouse model

Taking into account the obtained results and that there wasn't any other available sgRNA for spCas9, we decided to switch to an all in one system. Using the *Streptococcus Aureus Cas9* (SaCas9) we were able to design a single plasmid containing the sgRNA, the Donor, the human U6 promoter and the SaCas9 (fig.11). The activation of the plasmid inside the cells was confirmed by the expression of an EGFP fluorescence .

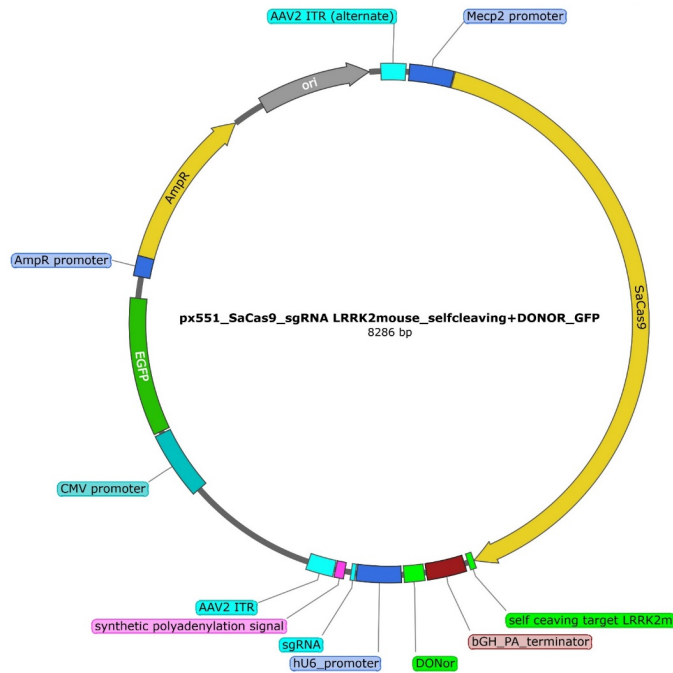


Fig.11: the SaCas9 plasmid design. The all in one plasmid system design is shown. The plasmid is composed by the SaCas9 coding sequence (in yellow) under the control of MECP2 promoter (blue); the Donor is evidenced in green and the sgRNA in light blue. The EGFP fluorescent reporter CDS is located outside from the ITR (light blue).

In order to evaluate the transfection efficiency of this new plasmid we performed a preliminary transfection experiment in mutated mouse fibroblasts. 48h after transfection, the green fluorescence was assessed by FACS analysis. As expected, no EGFP + cells were present in the negative control (fig.12) while we got 39.6% of EGFP + cells in the positive control (fig.12) transfected with the EGFP plasmid. For the sample transfected with the correction plasmid, 12.8% of green cells were observed (fig.12).

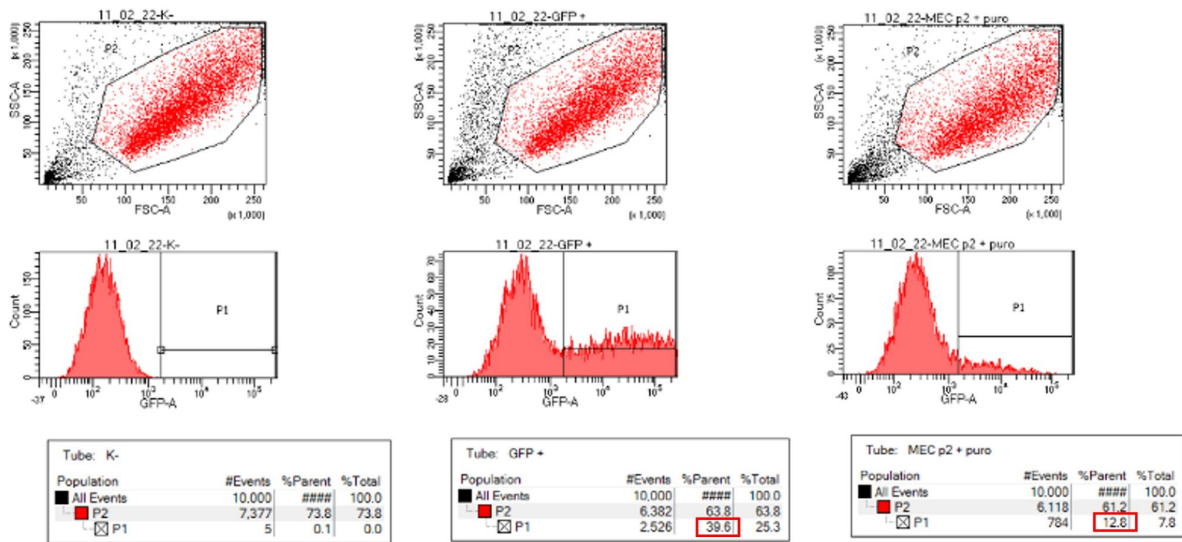


Fig.12: FACS analysis on transfected mouse fibroblasts. 48h post transfection, EGFP fluorescence was estimated by FACS analysis. From the left side are shown: the negative control, the positive control, and the treated sample.

Based on this result, a new editing experiment with the all in one plasmid was carried out. EGFP + cells were already visible 24 hours after the transfection. 48 hours later the EGFP + cells were recovered by FACS and the DNA was extracted and analyzed by NGS in order to characterize the targeted DNA region and to estimate the obtained HDR level. BAM and BAI files obtained from the NGS were uploaded into the Integrative Genomics Viewer (IGV) (<https://software.broadinstitute.org/software/igv/>) to verify the replacement of the mutated base and the presence of indel events in the neighboring sites. Results demonstrated that no correction was achieved (fig.13).

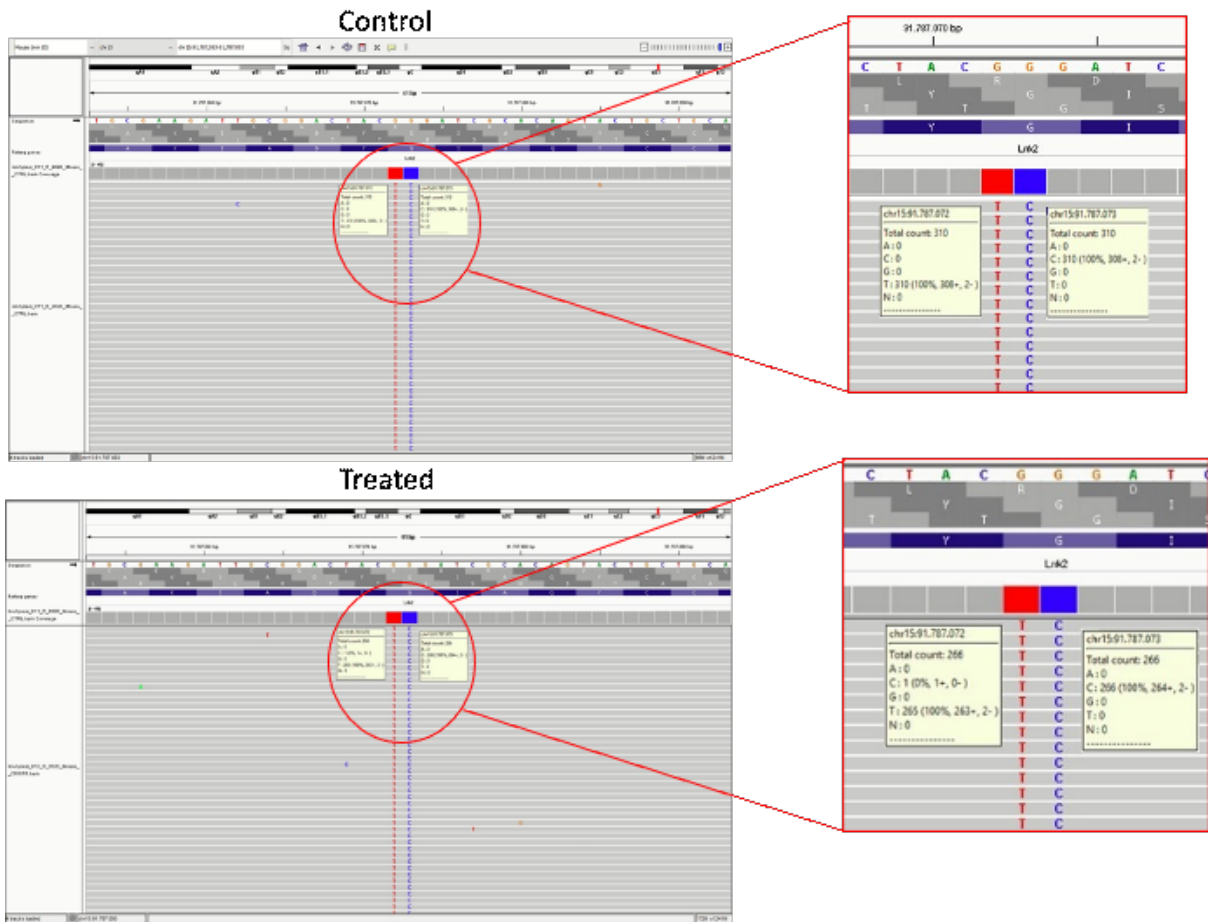


Fig.13: IGV analysis of treated mouse fibroblasts. Representative image of control and treated sample of mouse fibroblasts. The control (upper panel) and the treated (lower panel) samples are indistinguishable, indicating that no correction was achieved..

Following these results we decided to verify the expression of the SaCas9 in the mouse fibroblasts with Western Blot (WB) analysis. WB was performed on whole protein extract isolated from mouse fibroblasts and HEK293 cells both transfected with the SaCas9 plasmid. No expression of the protein was detected in fibroblasts (fig.14).

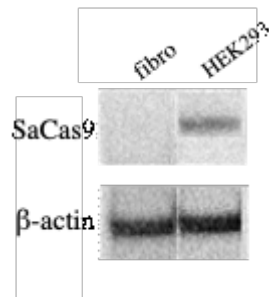


Fig.14: Western Blot analysis for SaCas9 expression. Western blot analysis for SaCas9 on HEK293 cells and mouse fibroblasts shows the presence of the protein exclusively in the HEK293 cells (right). β -actin was used as loading control.

4.3.1.2 Changing the promoter for the mouse model.

Considering the absence of expression of SaCas9 in mouse fibroblasts, we substituted *MECP2* promoter with a stronger one: the EF1 α promoter [102]. Furthermore a puromycin resistance cassette, outside from the ITR, was added to the previous design (fig.15) in substitution of the EGFP cassette (fig.12).

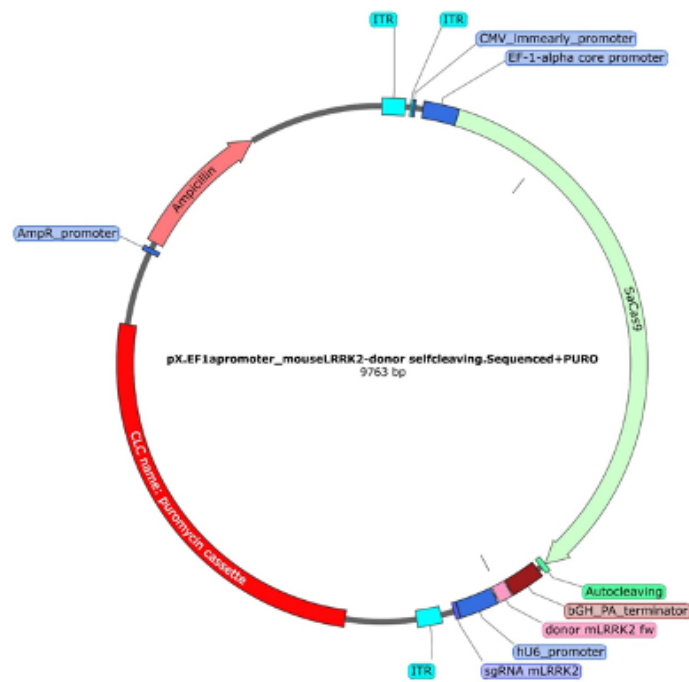


Fig.15: The new plasmid design with ef1 α promoter. The SaCas9 coding sequence (light green) is located under the control of the strong EF1 α promoter (dark blue). The puromycin resistance cassette is located outside from the ITR.

After cloning this new promoter inside the plasmid, we performed a Sanger sequencing in order to verify its correct insertion in the backbone. Sanger sequencing demonstrated that the promoter was correctly inserted (fig.16) and there were no indels in the surrounding regions.

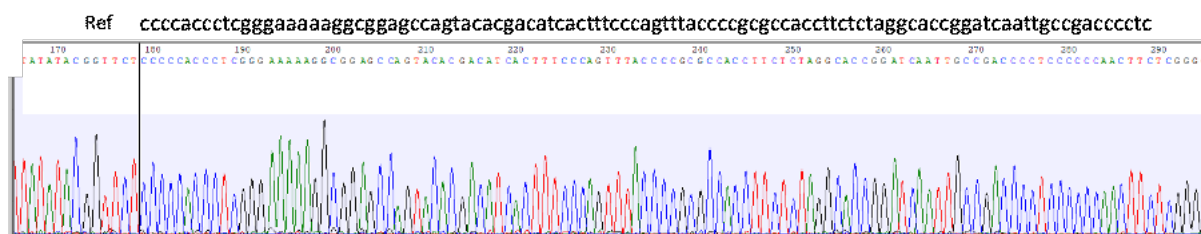


Fig.16: Sanger sequencing for the insertion of the promoter. The promoter reference sequence is shown above the chromatogram.

Subsequently, we determined the most suitable puromycin concentration to select the cells that have correctly incorporated the new plasmid by performing a puromycin killing curve experiment. Mouse primary fibroblasts were transfected with a puromycin resistance plasmid (Addgene #22814); 48h post transfection 1,2,5,10 ug/mL of puromycin was added to the culture. Cell death was visually evaluated with a light microscope after 48 (fig.17a) and 72h (fig.17b). 48 hours after the beginning of the selection with puromycin, the cells treated with 10 ug/mL were all dead; we continued the selection with the other puromycin concentrations up to 72h. The survival rate of the cells made us select the concentration of 5ug / mL as the most suitable for our purposes (fig.17b).

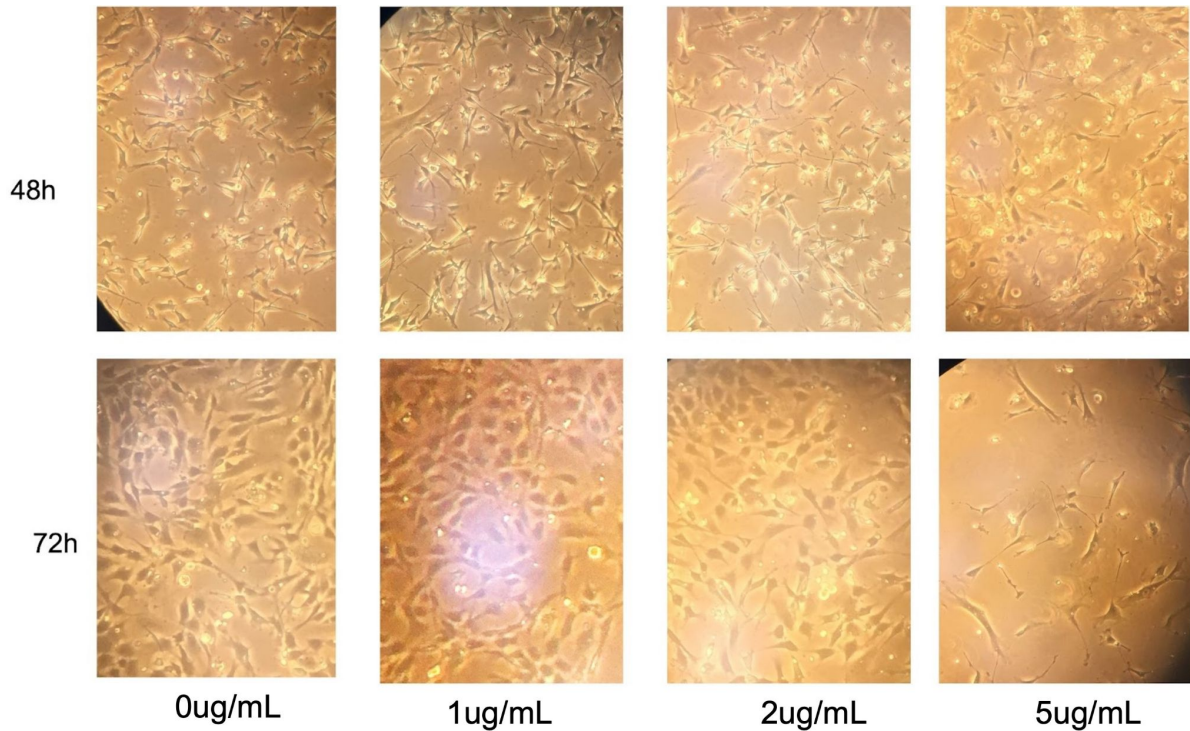


Fig.17: Puromycin killing curve. Representative images of the selection carried out at different puromycin concentrations. a) Pictures taken 48 hours after the beginning of the selection.+ b) Pictures taken 72 hours after the beginning of the selection. From the left to the right we have 0ug/mL; 1ug/mL; 2ug/mL and 5ug/mL puromycin.

Considering these results, we carried out a new editing experiment. 48 hours post transfection, cells have been treated with 5ug/mL of puromycin. 48 hours later, DNA has been extracted. NGS deep sequencing experiment is ongoing.

4.3.2 The human model

For the human model we have chosen the XCas9 (Addgene #108279) to target the c.6055G>A(p.(G2019S)) mutation. Due to the XCas9 size, we have selected a dual plasmid approach. The first plasmid encodes the Cas9 protein flanked by two target sequences (fig. 19b). The second one is composed by the sgRNA under the control of the U6 promoter, a WT Donor of 500bp, and the mCherry/eGFP reporter system as described above (fig.6).

In order to assess the functionality of our design we made a preliminary transfection test on these cells with a negative control (fig.18a), transfected with an empty plasmid, an EGFP + control (fig.18b) and two samples transfected with both plasmids (biological replicates) (fig.18 lower panel). 48 hours post transfection red and green fluorescence was assessed by FACS (fig.18).

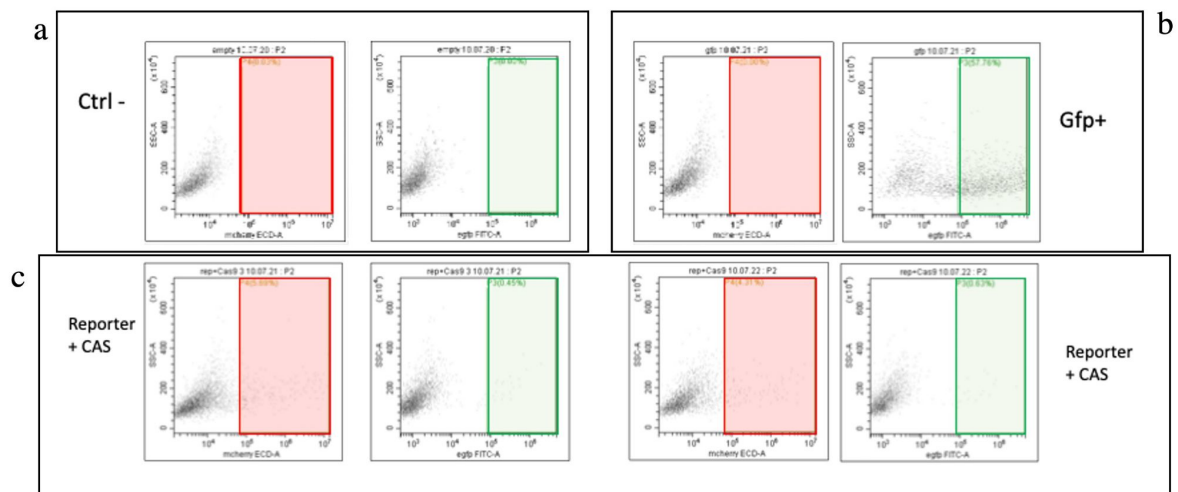


Fig.18: FACS analysis in primary fibroblasts. FACS analysis on human primary fibroblasts. In the upper left panel (a) the negative control is shown; the upper right panel (b) shows the EGFP + control; the lower panels (c) show duplicate samples transfected with both the Reporter and the Cas9 plasmids.

Neither red nor green cells were found in the negative control (fig.18a); for the positive control, transfected with an EGFP plasmid, we obtained 57.76% of EGFP + cells (fig.18b). For the two edited samples, 5,69% of red cells were obtained 0.45% of which were also green (fig.18c).

In order to further analyze this low efficiency, and to verify the presence of some differences with a different method, we carried out a WB analysis in control, mutated and treated cells (fig.19a) evaluating the expression of the EGFP, together with the expression of the total level of LRRK2 protein (fig.19b).

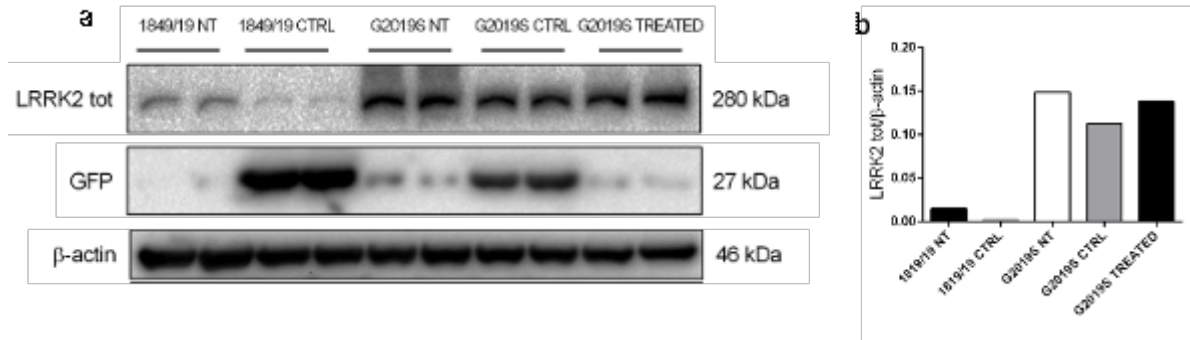


Fig.19: WB analysis in control and treated human primary fibroblasts. WB analysis in control, non-treated and treated human primary fibroblasts is shown. β -actin was used as loading control. On the left (a) the image of the nitrocellulose membrane with two WT controls, (non treated and treated) and three mutated samples (not treated, EGFP + control and treated with the correction plasmids); from the bottom, LRRK2, GFP and β -actin blots are shown for each sample. On the right (b) the analysis of the total expression levels of LRRK2. The values on the y axis are the averages of percentage of proteins relative to WT normalized to β -Actin expression. The analysis has been done in collaboration with the University of Ferrara.

Total LRRK2 levels are higher in the mutant samples with respect to the control one (Fig.19a,b). No difference between treated and untreated mutated cells was observed. For what concern the expression of EGFP, we confirmed it is expressed in the treated cells, although at low levels.

Therefore, we decided to proceed with an editing experiment. After transfection, both the control and the treated DNA were analyzed using NGS. BAM and BAI files obtained from the NGS were uploaded into the IGV. No correction was observed in the treated sample compared to the control one (fig.20).

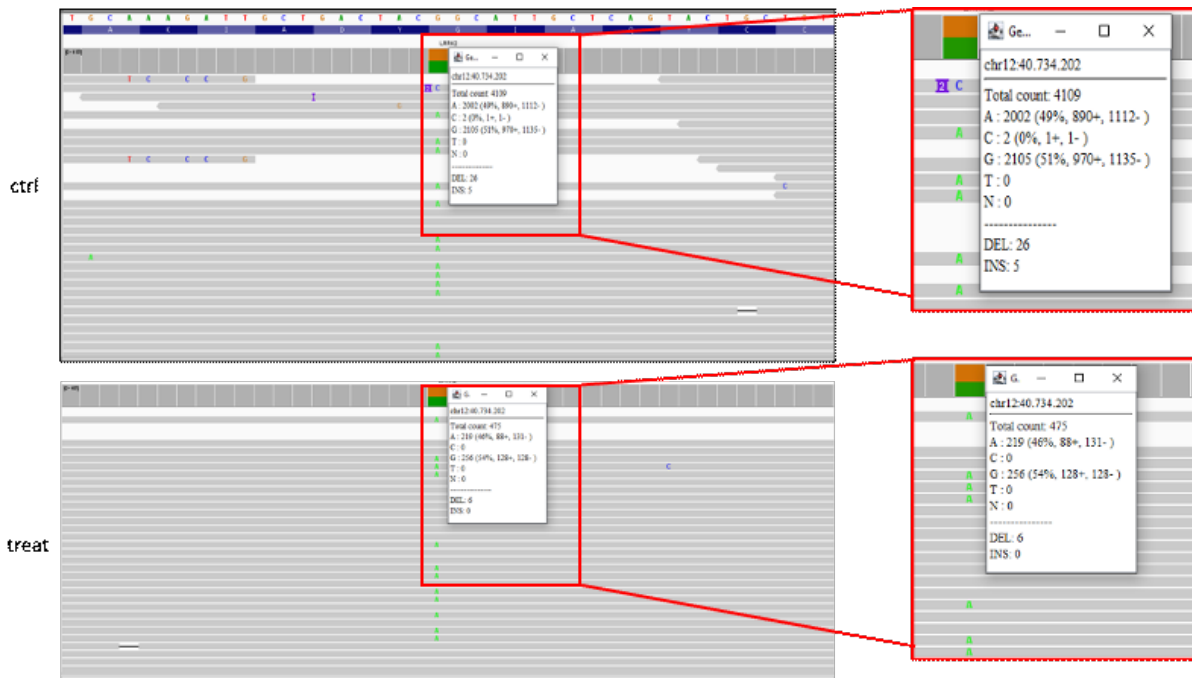


Fig.20: IGV analysis of the NGS experiment. IGV analysis on both control (upper) and treated (lower) samples are shown in the image. No correction is present.

4.3.2.1 Adenine Base Editor for human PD model

Taking into account the previous results, we decided to test a new strategy for our mutation: the Adenine base editor (ABE) approach.

We designed a dual plasmid approach with a first plasmid carrying the ABE system (Addgene #108382) (fig.21a) and a second one carrying the sgRNA under the human U6 promoter. (fig.21b). The presence of the plasmid inside the cell is confirmed by a fluorescent reporter system with the EGFP CDS under the control of the CMV promoter (fig.21b).

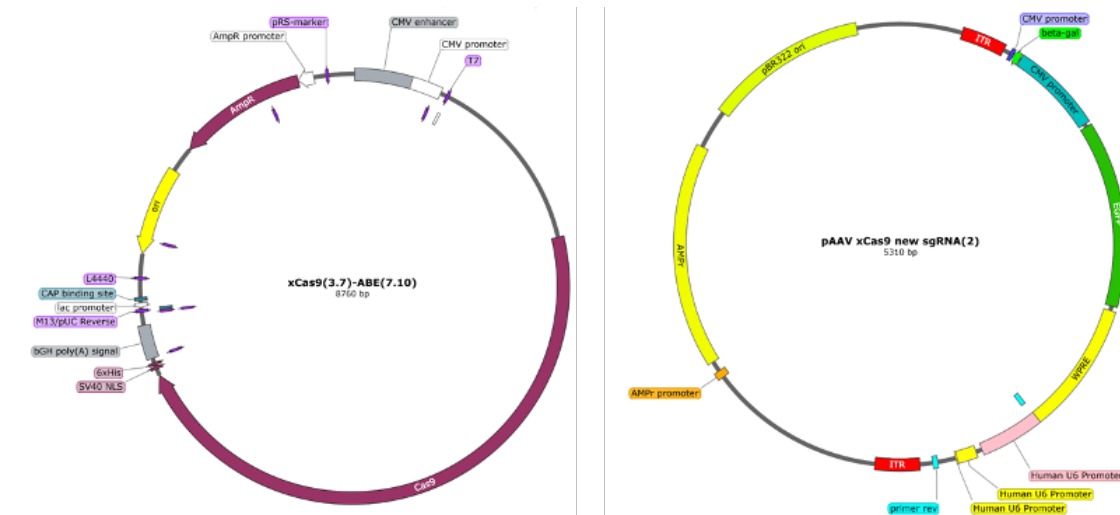


Fig.21: the ABE plasmid design. On the left side (a) the plasmid carrying the ABE system that was obtained from Addgene; on the right side (b) the plasmid with the sgRNA and the eGFP fluorescent reporter system under the CMV promoter.

In order to test the ABE system, we performed a first preliminary transfection test. 24 hours later, EGFP + cells were already visible under the microscope (Fig 22a) while 48 hours later, green fluorescence was assessed by FACS (Fig 22b) resulting in 26% of EGFP + cells.

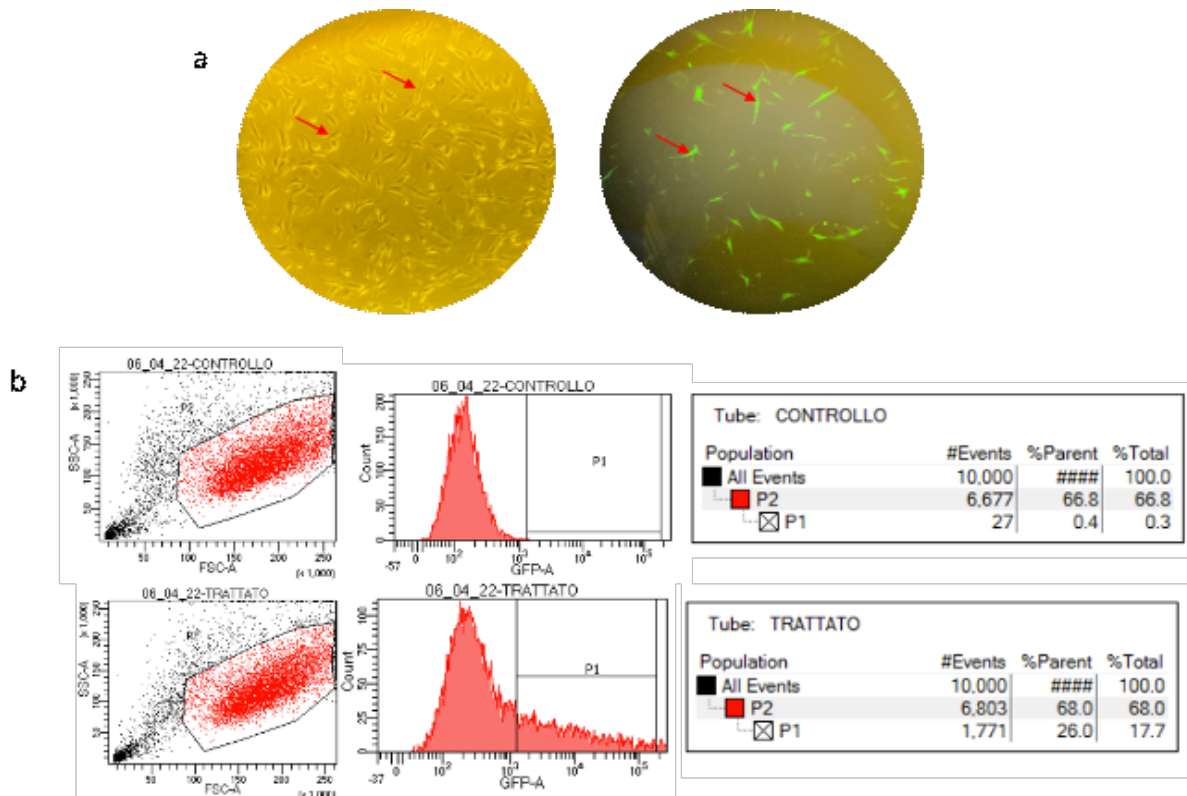


Fig.22: Microscope and FACS analysis of the transfected fibroblasts. Preliminary transfection experiment results are shown. a) Fluorescence microscope image of the transfected fibroblasts taken 24 hours after

transfection; the red arrows evidence the same cell under light and fluorescent microscopy, showing EGFP expression. b) FACS analysis results on both control and treated sample.

Based on this result, we performed a first editing experiment. For the selection of the transfected cells, a third plasmid, encoding puromycin resistance (Addgene #22814), was added to the mix.

48 hours post transfection, cells have been treated with 5ug/mL of puromycin, determined as described above (fig.17). 24 hours after the beginning of the selection the DNA was extracted and an NGS sequencing was performed. BAM and BAI files for both control and treated samples were uploaded on the IGV. (Fig.23). The analysis showed no base replacement in the treated sample (fig.23b). To further analyze the targeted region we uploaded the FASTQ files from control and treated samples to an online analysis tool: the BE analyzer, a javascript based tool for NGS data of CRISPR base edited cells (<http://www.rgenome.net/be-analyzer/>) [102]. The BE analysis confirmed that no substitution was present in the treated sample with respect to the control one (Fig 23).

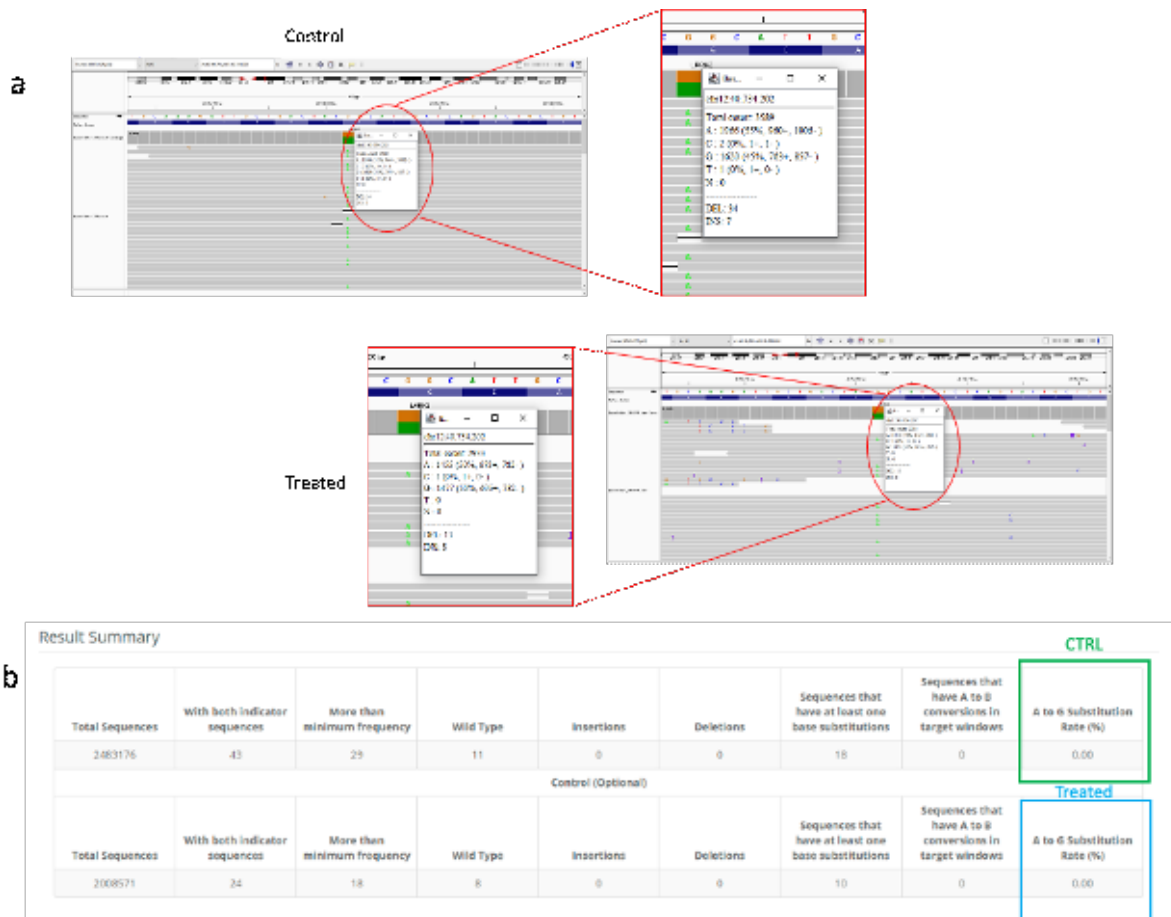


Fig.23: ABE results. ABE experiment results are shown; in the upper panel (a) the IGV image of both the control (up) and treated (down) samples. In the lower panel (b) the obtained results from the BE analyzer online tool.

4.3.2.2 SpCas9 strategy for G2019S mutation.

Considering the negative results with both saCas9 and BE, we designed another strategy with the help of MIT CRISPR Design Tool (<http://crispr.mit.edu>). We selected two different sgRNAs that overlap on the mutation site (fig.24a) and we set up a new dual plasmid strategy composed by a first plasmid which carry the SpCas9 under the control of the CMV promoter (fig.24b) and a second one which carries the two sgRNAs under the U6 promoter and a 1kb donor (fig.24c). The expression of the plasmid inside the cell can be confirmed by EGFP expression (fig.24c).

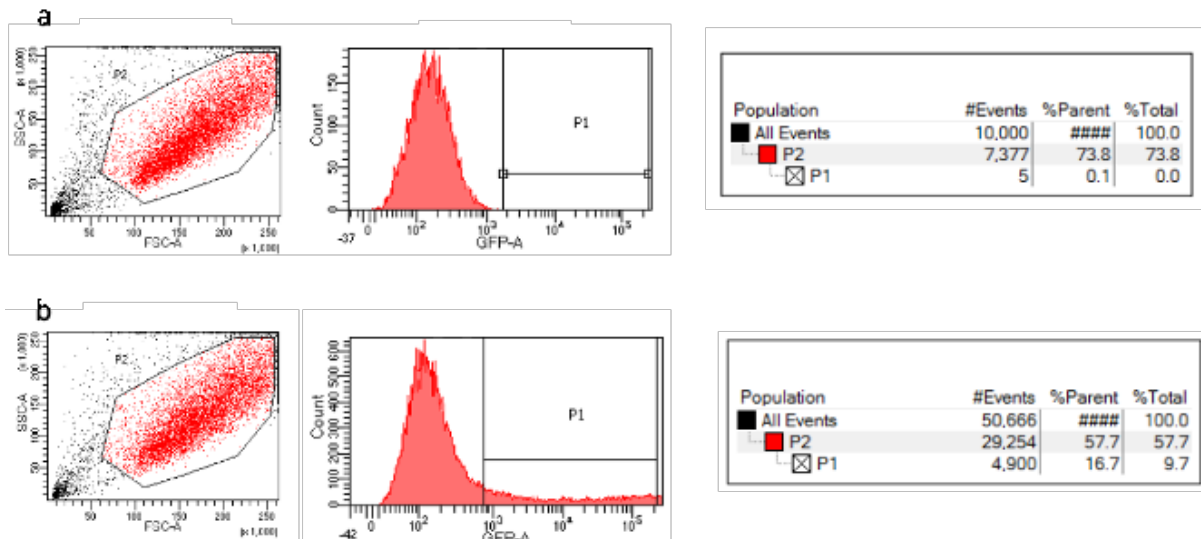
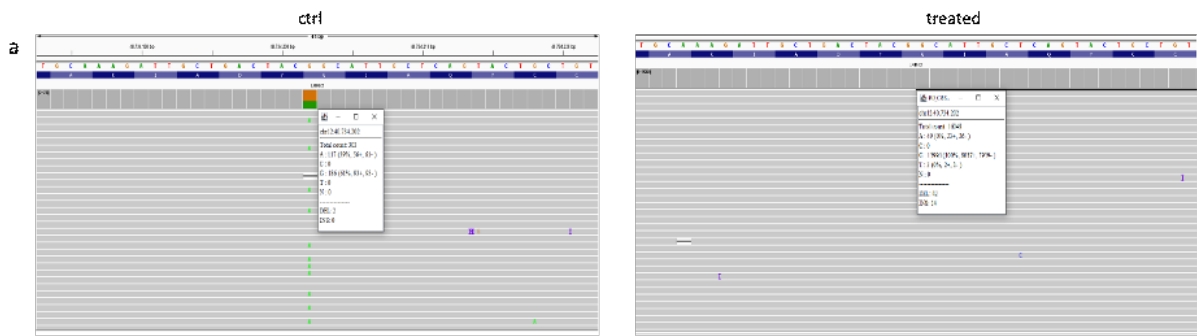


Fig.25: Preliminary FACS analysis on primary fibroblasts. a) the negative control, transfected with an empty plasmid ; b) the treated sample, transfected with both the Reporter and the Cas9 plasmids.

For the selection of the transfected cells, we used again a third plasmid which express the antibiotic resistance. 48 hours post transfection, the DNA was extracted and analyzed by NGS. For both control and treated sample, the BAM and BAI files were loaded on the IGV and the replacement of the base was inspected together with possible indels (fig.26a). FASTQ files from treated and control samples were loaded on CasAnalyzer to visualize the percentage of homology directed repair (HDR). In this case our system resulted to be efficient (fig.26b) with an HDR of 75%.



b

WT sequence
(blue: indicator sequences at each ends of comparison range, green: crRNA sequence, red: WT marker sequence)

AAAGCATACCTTCTCTGTATATAGACTATATGTTTGTATCTCTCTCAATATCTCTTAAAGGGAAGAGTGGACAGAGATTTTGTGCTTGCATAGTGGACATTTATATTAAAGAAATGGACAAAATATTATATATATACAT
TTGANTAGATTTCTCTGTATTTCTGGGACATCTCCACTGAGCCATGATATATCCGAGACTGGAAACCCGAACTGTCTCTCTTTCTGACTGTATGGCAATGCTGCTGACTACGACATTCCTCATTCCGAAAGATTG

crRNA sequence
GACTACGACATTCCTCATTCCGAAAGATTG

Comparison range (bp)	Minimum Frequency (10%)	WT marker (bp)
15	1	0

Run again with different values.

Total Sequences	With both indicator sequences	More than minimum frequency	Insertions	Deletions	0.4 ins/del alleles		75.2% perfect edited alleles	
					indel frequency	indel frequency	HDR frequency	HDR frequency
222251	101	140	0	0	0 (0.0%)	0 (0.0%)	90 (62.1%)	
976368	7763	7755	12	0	12 (0.2%)	12 (0.2%)	7735 (99.7%)	

Fig.26: Efficient editing is reached on primary fibroblasts. a) NGS results for edited fibroblasts. On the left side the control and on the right the treated sample, with the replacement of the correct base, is shown. b) CasAnalyzer results evidencing the 75% of perfect edited alleles.

5. Discussion and future perspectives

Parkinson's disease is a slowly progressive neurodegenerative disorder of the nervous system which mainly affects the motor system. It is characterized by tremor, stiffness, slowing of voluntary movements and difficulty in maintaining balance; a subset of patients also display cognitive impairment [1]. Several mutations associated with PD have been identified in Leucine Rich Repeat Kinase 2 (*LRRK2*) gene; among them, the most common is the hotspot p.Gly2019Ser (c.6055G>A) variant.

Despite the growing interest in this field, no definitive treatment is available; Levodopa coupled with Carbidopa unfortunately are only able to slow down the progression of the disease. These treatments indeed present an efficacy which decreases during time, requiring a progressive increase of the drug dosage in order to reduce the symptoms. Unfortunately, in about 5 years from the starting of the treatment, the maximum dosage that can be administered is reached. As a consequence, symptoms are no longer under control. Moreover, these treatments suffer from different important side effects, such as fluctuation, dyskinesias or toxicity [103]. In young patients also deep brain stimulation (DBS) is proposed as a possible therapy. [104]

For PD linked to *LRRK2* mutations, which result in Serin1292 hyper-phosphorilation, the possibility to achieve a successful therapy comes out with *LRRK2* kinase inhibitors, which are currently in phase IIb clinical trials. These molecules have been designed to counterbalance the increased *LRRK* kinase activity and have the advantage of having a good brain permeability with the capacity to efficiently cross the BBB. Kinase inhibitors have resulted to be neuroprotective in preclinical models of PD. [105] Actually, published data show that kinase inhibitors have the potential to correct lysosomal dysfunction in patients with PD at a dosage which is generally well tolerated [106] However, they present important selectivity problems

and side effects, especially in lungs and kidneys. Moreover, LRRK2 protein degradation has been also reported in animal models.[107,108]

In this scenario, gene therapy seems to be a very promising alternative approach to provide a definitive therapy for PD. In the past years, it has been demonstrated how the CRISPR/Cas9 bacterial immune system can be engineered, becoming an efficient solution to revert disease causative variants and, therefore, to cure genetic disorders [69,70]. Moreover, our group has previously published the feasibility of the application of CRISPR/Cas9 system for different genetic disorders both in human primary fibroblasts, iPSC-derived neurons and in podocyte lineage cells [71,72,87]. Taking into account these premises, the overall goal of this work is the application of CRISPR/Cas9-based gene editing for the correction of the hotspot c.6055G>A (p.(Gly2019Ser)) variant in *LRRK2* gene.

The fact that the brain is our target organ is quite challenging for obvious reasons. However, considering the important limitations and of available treatments, if we would be able to identify the patients harbouring LRRK2 mutations prior to disease manifestation, we could potentially be able to correct the mutation before the onset of the disease and thus prevent, or significantly delay, neuronal damage and symptoms onset. Indeed, even if our approach should not correct 100% of the cells,, a partial correction could be enough to delay disease progression so that treatment with Levodopa and Carbidopa will start belatedly and the maximum dosage of administrable drug might not be reached allowing a better management of the condition and an important amelioration in patients quality of life.

Based on our previous results and different studies demonstrating that it is possible to apply the CRISPR/Cas9 gene editing approach in human primary fibroblasts [109], we decided to validate our approach in primary fibroblasts obtained from a mutated patient and from the KI mouse model harbouring the corresponding mutation. In order to apply the system both in

mouse and in human primary fibroblasts we selected two different guides. The choice to use different sgRNAs and Cas9 for the animal and human model derives from the fact that in the mouse genome two adjacent nucleotides have been mutated in order to obtain the same aminoacid substitution present in the patients: GGG becomes TCG, affecting the first and second bases of the triplet [110].

For the mouse model, we started to test the strategy using a dual plasmid approach with a first plasmid carrying the *Streptococcus pyogenes* Cas9 (SpCas9) and a second one which carries the sgRNA, a donor DNA and a specifically designed fluorescent mCherry-EGFP fusion protein that allows the quantification and the selection of the cells through flow cytometry. Our system revealed 17% of EGFP positive cells which in a second independent experiment decreased to 0.1%. A successive test confirmed again a very low percentage of green cells (0,45%). This could be explained by a low efficiency of the Cas9 to cleave the target sequence between the two fluorescent markers (mCherry-EGFP). In our previous works on Rett and Alport syndrome we have demonstrated that this double reporter system strategy is effective and we could recover a good percentage of EGFP positive cells. However, the real efficiency of this cut is not predictable and it might be influenced from the specific target sequence or from other features influencing the accessibility of the sequence in the specific plasmid. Moreover, we must also consider the hypothesis that a self-cut could preferentially occur on the plasmid harbouring the Cas9 itself and not on the Reporter plasmid. Finally, we can not rule out the possibility that the selected sgRNA, there only available for spCas9 on the mutated sequence, is not efficient in driving Cas9 to the mutated target sequence. For these reasons, we switched to an “all in one” plasmid. The generation of a single plasmid is possible thanks to the small size of the SaCas9, which leaves enough space inside the plasmid for the insertion of the sgRNA, the Donor DNA and a selection system. Moreover, the SaCas9 has been proved to be able to edit the genome with an efficiency which is equiparable to the SpCas9 being 1kb

shorter [111]. Unfortunately, despite a good preliminary test showing 12.8% of EGFP + cells, NGS analyses didn't evidence any base replacement. This could be explained by the absence of SaCas9 expression in the mouse fibroblasts as shown by the WB analysis. This can be justified by literature findings which underline that the selected Mesp2 promoter has a low expression in mouse fibroblasts [112]. We thus decided to substitute the Mesp2 promoter with the stronger EF1a promoter which is reported to drive strong gene expression in different cell types including fibroblasts [113]. The correct insertion of the promoter in the plasmid backbone was confirmed by Sanger sequencing. Further analyses are ongoing to verify the effective correction ability of this new design.

For the human model, the only sgRNA that we could design on the mutated sequence was for the XCas9 variant which recognizes an NG PAM sequence [101]. The XCas9 shows promising potential in improving targeting specificity and broaden the target range of the system. It exhibit an almost equivalent editing efficiency compared to the canonical SpCas9 [114]. Due to the large dimension of the XCas9, also in this case we decided to split the system into 2 plasmids composed by a reporter plasmid with the sgRNA, the Donor and the dual mCherry-eGFP fluorescent reporter, and a second one carrying the Xcas9. The system resulted to be inefficient in targeting and correcting the desired locus.

Literature findings have demonstrated that Adenine Base editor (ABE) has the ability to efficiently convert a targeted A•T base pair into G•C [89]. Moreover *Chang K. et al* have recently demonstrated that this system is able to revert the p.Gly2019Ser mutation in iPSCs with a 24.5% of correction [115]. Following these published results, we decided to test in our cells the XCas9 ABE system with a dual plasmid approach. The difference with the other experiments resides in the fact that the correction system doesn't need a donor DNA. This change can be easily explained by the different chemistry used for the correction. In fact, in ABE a modified deoxyadenosine deaminase is used together with a functioning one for the

conversion of the Adenine (A) to an inosine (I) which is recognized by the polymerase system as Guanosine (G). This could make the system able to efficiently revert our hotspot p.Gly2109Ser mutation. However, despite the 26 % of EGFP + transfected cells found in preliminary tests, this system wasn't able to edit p.Gly2019Ser mutation. This is in contrast to results reported by Chang and colleagues, that obtained an efficient correction. However, we must consider that they worked on different cells, namely iPSCs. Many factors, including different chromatin accessibility in different cell types, different capacity to efficiently express the plasmid or different plasmid design, might explain this difference and additional studies are surely needed to assess the real potential of ABE base editor for the correction of the p.Gly2109Ser LRRK2 variant.

In parallel, we have decided to also try to use SpCas9. For this new strategy we designed two different overlapping sgRNAs, positioned at the opposite ends of the mutation. These two sgRNA were inserted into a reporter plasmid containing an EGFP reporter and a 1kb Donor. A large Donor has been selected in order to try to increase the correction efficiency of the system. The SpCas9 was expressed by a second plasmid. Results with this approach demonstrated 75% of perfect corrected alleles. Additional experiments are ongoing to validate this extremely positive result.

In conclusion, our findings proved that our gene-editing based approach could effectively be used to target and correct the pathogenic variant c.655G>A p.Gly2019Ser in *LRRK2* gene. This represents a promising starting point for the development of a new therapeutic approach for PD. Future studies will be focused on the confirmation of these results in dopaminergic neurons derived from induced pluripotent stem cells (iPSCs).

6. Bibliography

1. Samii, A., Nutt, J. G., & Ransom, B. R. (2004). Parkinson's disease. *Lancet* (London, England), 363(9423), 1783–1793
2. Wakabayashi, K., Tanji, K., Odagiri, S., Miki, Y., Mori, F., & Takahashi, H. (2013). The Lewy body in Parkinson's disease and related neurodegenerative disorders. *Molecular neurobiology*, 47(2), 495–508.
3. Spillantini MG, Schmidt ML, Lee VM, et al. Alpha-synuclein in Lewy bodies. *Nature* 1997;388:839–40
4. Burre J, Sharma M, Sudhof TC. Cell Biology and Pathophysiology of alpha-Synuclein. *Cold Spring Harbor perspectives in medicine*. 2018. March 1;8
5. Poewe, W., Seppi, K., Tanner, C. et al. Parkinson disease. *Nat Rev Dis Primers* 3, 17013 (2017).
6. Xilouri M, Brekk OR, Kirik D, et al. LAMP2A as a therapeutic target in Parkinson's disease. *Autophagy*. 2013;9(12):2166–2168
7. Alvarez-Erviti L, Rodriguez-Oroz MC, Cooper JM, et al. Chaperone-mediated autophagy markers in Parkinson disease brains. *Arch Neurol*. 2010;67(12):1464–1472.
8. Obeso, J. A., Rodríguez-Oroz, M. C., Benitez-Temino, B., Blesa, F. J., Guridi, J., Marin, C., & Rodriguez, M. (2008). Functional organization of the basal ganglia: therapeutic implications for Parkinson's disease. *Movement disorders : official journal of the Movement Disorder Society*, 23 Suppl 3, S548–S559.
9. Marsden C. D. (1990). Parkinson's disease. *Lancet (London, England)*, 335(8695), 948–952.
10. Dickson DW ,Braak H ,Duda JE ,Duyckaerts C ,Gasser T ,Halliday GM ,Hardy J ,Leverenz JB ,Del Tredici K ,Wszolek ZK ,Litvan I.

- Neuropathological assessment of Parkinson's disease: refining the diagnostic criteria. *Lancet Neurol* 2009;8:1150–7
11. Jankovic J. Parkinson's disease: clinical features and diagnosis. *J Neurol Neurosurg Psychiatry*. 2008;79(4):368–376
 12. Tolosa, E., Garrido, A., Scholz, S. W., & Poewe, W. (2021). Challenges in the diagnosis of Parkinson's disease. *The Lancet. Neurology*, 20(5), 385–397
 13. Hoehn MM, Yahr MD. Parkinsonism: onset, progression and mortality. *Neurol.*, 1967; 17: 427–442
 14. LeWitt P. A. (2015). Levodopa therapy for Parkinson's disease: Pharmacokinetics and pharmacodynamics. *Movement disorders : official journal of the Movement Disorder Society*, 30(1), 64–72.
 15. Balestrino, R., & Schapira, A. (2020). Parkinson disease. *European journal of neurology*, 27(1), 27–42.
 16. Deng, Hao, Peng Wang, and Joseph Jankovic. "The genetics of Parkinson disease." *Ageing research reviews* 42 (2018): 72-85
 17. Puschmann A. (2017). New Genes Causing Hereditary Parkinson's Disease or Parkinsonism. *Current neurology and neuroscience reports*, 17(9), 66
 18. Polymeropoulos MH, Lavedan C, Leroy E et al. Mutation in the alpha-synuclein gene identified in families with Parkinson's disease. *Science* 1997; 276: 2045–7
 19. Rüger R et al. Ala30Pro mutation in the gene encoding alpha-synuclein in Parkinson's disease. *Nat. Genet* 18, 106–108 (1998)
 20. Zarranz JJ et al. The new mutation, E46K, of alpha-synuclein causes Parkinson and Lewy body dementia. *Ann. Neurol* 55, (164–173)

21. Appel-Cresswell S et al. Alpha-synuclein p.H50Q, a novel pathogenic mutation for Parkinson's disease. *Mov. Disord* 28, (811–81)
22. Lesage S et al. G51D α -synuclein mutation causes a novel parkinsonian-pyramidal syndrome. *Ann. Neurol* 73, 459–471
23. Pasanen P et al. Novel alpha-synuclein mutation A53E associated with atypical multiple system atrophy and Parkinson's disease-type pathology. *Neurobiol. Aging* 35, 2180.e1–2180.e5 (2014)
24. Mazzulli JR, Xu Y-H, Sun Y, Knight AL, McLean PJ, Caldwell G, Sidransky E, Grabowski G & Krainc D (2011) Gaucher disease glucocerebrosidase and α -synuclein form a bidirectional pathogenic loop in synucleinopathies. *Cell* 146, 37–52
25. Kasten M, Hartmann C, Hampf J, et al. Genotype-phenotype relations for the Parkinson's disease genes Parkin, PINK1, DJ1: MDS Gene systematic review. *Mov Disord* 2018; 33: 730–41
26. Matsuda N, Sato S, Shiba K, Okatsu K, Saisho K, Gautier CA, Sou YS, Saiki S, Kawajiri S, Sato F, et al. PINK1 stabilized by mitochondrial depolarization recruits Parkin to damaged mitochondria and activates latent Parkin for mitophagy. *J Cell Biol.* 2010;189:211–221
27. Geisler S, Holmstrom KM, Skujat D, Fiesel FC, Rothfuss OC, Kahle PJ, Springer W. PINK1/Parkin-mediated mitophagy is dependent on VDAC1 and p62/SQSTM1. *Nat Cell Biol.* 2010a;12:119–131
28. Lesage S, Drouet V, Majounie E, Deramecourt V, Jacoupy M, Nicolas A, et al. Loss of VPS13C function in autosomal-recessive parkinsonism causes mitochondrial dysfunction and increases PINK1/parkin-dependent mitophagy. *Am J Hum Genet.* 2016;98(3):500–513

29. Rudakou, U., Ruskey, J. A., Krohn, L., Laurent, S. B., Spiegelman, D., Greenbaum, L., Yahalom, G., Desautels, A., Montplaisir, J. Y., Fahn, S., Waters, C. H., Levy, O., Kehoe, C. M., Narayan, S., Dauvilliers, Y., Dupré, N., Hassin-Baer, S., Alcalay, R. N., Rouleau, G. A., Fon, E. A., ... Gan-Or, Z. (2020). Analysis of common and rare VPS13C variants in late-onset Parkinson disease. *Neurology. Genetics*, 6(1), 385
30. Eiyama, A., & Okamoto, K. (2015). PINK1/Parkin-mediated mitophagy in mammalian cells. *Current opinion in cell biology*, 33, 95–101
31. Hancock-Cerutti, W., Wu, Z., Xu, P., Yadavalli, N., Leonzino, M., Tharkeshwar, A. K., Ferguson, S. M., Shadel, G. S., & De Camilli, P. (2022). ER-lysosome lipid transfer protein VPS13C/PARK23 prevents aberrant mtDNA-dependent STING signaling. *The Journal of cell biology*, 221(7), e202106046
32. Vidyadhara DJ, Lee JE, Chandra SS. Role of the endolysosomal system in Parkinson's disease. *J Neurochem*. 2019 Sep;150(5):487-506.
33. Marin I. Ancient origin of the Parkinson disease gene LRRK2. *J Mol Evol*. 2008;67:41–50.
34. Gilsbach BK, Kortholt A. Structural biology of the LRRK2 GTPase and kinase domains: implications for regulation. *Front Mol Neurosci*. 2014;7:32.
35. Sen S, Webber PJ, West AB (2009) Dependence of leucine-rich repeat kinase 2 (LRRK2) kinase activity on dimerization. *J Biol Chem* 284, 36346–36356
36. Anand VS, Braithwaite SP. LRRK2 in Parkinson's disease: biochemical functions. *FEBS J*. 2009;276:6428–6435
37. West AB, Moore DJ, Choi C, Andrabi SA, Li X, Dikeman D, Biskup S, Zhang Z, Lim KL, Dawson VL, Dawson TM. 2007. Parkinson's disease-associated

- mutations in LRRK2 link enhanced GTP-binding and kinase activities to neuronal toxicity. *Hum Mol Genet* 16:223–232.
38. Gardet A., Benita Y., Li C., Sands B.E., Ballester I., Stevens C. et al. (2010) LRRK2 is involved in the IFN-response and host response to pathogens. *J. Immunol.* 185, 5577–5585 10.4049/jimmunol.1000548
 39. Cook D.A., Kannarkat G.T., Cintron A.F., Butkovich L.M., Fraser K.B., Chang J. et al. (2017) LRRK2 levels in immune cells are increased in Parkinson's disease. *NPJ Parkinson's Dis.* 3, 11 10.1038/s41531-017-0010-8
 40. Thévenet J., Pescini Gobert R., Hooft van Huijsduijnen R., Wiessner C., Sagot Y.J. and Sozzani S. (2011) Regulation of LRRK2 expression points to a functional role in human monocyte maturation. *PLoS One* 6, e21519 10.1371/journal.pone.0021519
 41. Hakimi M., Selvanantham T., Swinton E., Padmore R.F., Tong Y., Kabbach G., Venderova K., Girardin S.E., Bulman D.E., Scherzer C.R., LaVoie M.J., Gris D., Park D.S., Angel J.B., Shen J., Philpott D.J., Schlossmacher M.G. Parkinson's disease-linked LRRK2 is expressed in circulating and tissue immune cells and upregulated following recognition of microbial structures. *J. Neural Transm. (Vienna)* 2011;118(5):795–808
 42. Lee, H. S., Lobbstaël, E., Vermeire, S., Sabino, J., & Cleynen, I. (2021). Inflammatory bowel disease and Parkinson's disease: common pathophysiological links. *Gut*, 70(2), 408–417.
 43. Dzamko N. L. (2017). LRRK2 and the Immune System. *Advances in neurobiology*, 14, 123–143.
 44. Singleton AB, Farrer MJ & Bonifati V (2013) The genetics of Parkinson's disease: progress and therapeutic implications. *Mov Disord* 28, 14–23

45. Li, J. Q., Tan, L., & Yu, J. T. (2014). The role of the LRRK2 gene in Parkinsonism. *Molecular neurodegeneration*, 9, 47
46. Tolosa, E., Vila, M., Klein, C., & Rascol, O. (2020). LRRK2 in Parkinson disease: challenges of clinical trials. *Nature reviews. Neurology*, 16(2), 97–107.
47. Chai C, Lim KL. Genetic insights into sporadic Parkinson's disease pathogenesis. *Curr Genomics*. 2013 Dec;14(8):486-501
48. Shadrina MI, Illarioshkin SN, Bagyeva G, Bepalova EV, Zagorodskaja TB, Slominskii PA, Markova ED, Kliushnikov SA, Limborskaia SA, Ivanova-Smolenskaia IA: A PARK8 form of Parkinson's disease: a mutational analysis of the LRRK2 gene in Russian population. *Zh Nevrol Psikhiatr Im S S Korsakova*. 2007, 107: 46-50.
49. West A.B., Moore D.J., Biskup S., Bugayenko A., Smith W.W., Ross C.A. et al. (2005) Parkinson's disease-associated mutations in leucine-rich repeat kinase 2 augment kinase activity. *Proc. Natl. Acad. Sci. U.S.A.* 102, 16842–16847 10.1073/pnas.0507360102
50. Greggio E., Jain S., Kingsbury A., Bandopadhyay R., Lewis P., Kaganovich A. et al. (2006) Kinase activity is required for the toxic effects of mutant LRRK2/dardarin. *Neurobiol. Dis.* 23, 329–341
51. Berwick D.C., Javaheri B., Wetzel A., Hopkinson M., Nixon-Abell J., Grannò S. et al. (2017) Pathogenic LRRK2 variants are gain-of-function mutations that enhance LRRK2-mediated repression of β -catenin signaling. *Mol. Neurodegener.* 12, 9.
52. Singh F, Prescott AR, Rosewell P, Ball G, Reith AD, Ganley IG. Pharmacological rescue of impaired mitophagy in Parkinson's disease-related LRRK2 G2019S knock-in mice. *Elife*. 2021 Aug 3;10:e67604.

53. Gómez-Suaga P., Luzón-Toro B., Churamani D., Zhang L., Bloor-Young D., Patel S., et al. (2012). Leucine-rich repeat kinase 2 regulates autophagy through a calcium-dependent pathway involving NAADP. *Hum. Mol. Genet.* 21 511–525.
54. Rivero-Ríos P., Madero-Pérez J., Fernández B., Hilfiker S. (2016). Targeting the autophagy/lysosomal degradation Pathway in Parkinsons Disease. *Curr. Neuropharmacol.* 14 238–249.
55. Connor-Robson N., Booth H., Martin J. G., Gao B., Li K., Doig N., et al. (2019). An integrated transcriptomics and proteomics analysis reveals functional endocytic dysregulation caused by mutations in LRRK2. *Neurobiol. Dis.* 127 512–526.
56. Boecker, C. A., Goldsmith, J., Dou, D., Cajka, G. G., & Holzbaur, E. L. F. (2021). Increased LRRK2 kinase activity alters neuronal autophagy by disrupting the axonal transport of autophagosomes. *Current biology : CB*, 31(10), 2140–2154.e6.
57. Ishino Y, Shinagawa H, Makino K, et al. Nucleotide sequence of the iap gene, responsible for alkaline phosphatase isozyme conversion in *Escherichia coli*, and identification of the gene product. *J Bacteriol.* 1987;169:5429–5433.
58. Bolotin A, Quinquis B, Sorokin A, Ehrlich S (2005). “Clustered regularly interspaced short palindrome repeats (CRISPRs) have spacers of extrachromosomal origin.” *Microbiology* 151(8):2551-2561
59. Pourcel, C., G. Salvignol and G. Vergnaud (2005). "CRISPR elements in *Yersinia pestis* acquire new repeats by preferential uptake of bacteriophage DNA, and provide additional tools for evolutionary studies." *Microbiology* 151(Pt 3): 653-663

60. Barrangou R, Fremaux C, Boyaval P, et al. CRISPR provides acquired resistance against viruses in prokaryotes. *Science*. 2007;315:1709–1712
61. Wiedenheft B, Sternberg SH, Doudna JA. RNA-guided genetic silencing systems in bacteria and archaea. *Nature*. 2012;482:331–338.
62. Deltcheva E, Chylinski K, Sharma CM, et al. CRISPR RNA maturation by trans-encoded small RNA and host factor RNase III. *Nature*. 2011;471:602–607.
63. Garneau JE, Dupuis ME, Villion M, et al. The CRISPR/Cas bacterial immune system cleaves bacteriophage and plasmid DNA. *Nature*. 2010;468:67–71
64. Hryhorowicz, M., Lipiński, D., Zeyland, J., & Słomski, R. (2017). CRISPR/Cas9 Immune System as a Tool for Genome Engineering. *Archivum immunologiae et therapeuticae experimentalis*, 65(3), 233–240.
65. Hryhorowicz, M., Lipiński, D., Zeyland, J., & Słomski, R. (2017). CRISPR/Cas9 Immune System as a Tool for Genome Engineering. *Archivum immunologiae et therapeuticae experimentalis*, 65(3), 233–240.
66. Jinek, M., Chylinski, K., Fonfara, I., Hauer, M., Doudna, J. A., & Charpentier, E. (2012). A programmable dual-RNA-guided DNA endonuclease in adaptive bacterial immunity. *Science (New York, N.Y.)*, 337(6096), 816–821.
67. Mali, P., Yang, L., Esvelt, K. M., Aach, J., Guell, M., DiCarlo, J. E., Norville, J. E., & Church, G. M. (2013). RNA-guided human genome engineering via Cas9. *Science (New York, N.Y.)*, 339(6121), 823–826.
68. Luther DC, Lee YW, Nagaraj H, et al. Delivery Approaches for CRISPR/Cas9 Therapeutics in-vivo: Advances and Challenges. *Expert Opin Drug Deliv*. 2018 15:905-913

69. Frangoul, H., Altshuler, D., Cappellini, M. D., Chen, Y. S., Domm, J., Eustace, B. K., Foell, J., de la Fuente, J., Grupp, S., Handgretinger, R., Ho, T. W., Kattamis, A., Kernytsky, A., Lekstrom-Himes, J., Li, A. M., Locatelli, F., Mapara, M. Y., de Montalembert, M., Rondelli, D., Sharma, A., ... Corbacioglu, S. (2021). CRISPR-Cas9 Gene Editing for Sickle Cell Disease and β -Thalassemia. *The New England journal of medicine*, 384(3), 252–260.
70. Bengtsson NE, et al., Muscle-specific CRISPR/Cas9 dystrophin gene editing ameliorates pathophysiology in a mouse model for Duchenne muscular dystrophy. *Nat Commun*, 2017. 8: p. 14454
71. Croci, S., Carriero, M. L., Capitani, K., Daga, S., Donati, F., Papa, F. T., Frullanti, E., Lopergolo, D., Lamacchia, V., Tita, R., Giliberti, A., Benetti, E., Niccheri, F., Furini, S., Lo Rizzo, C., Conticello, S. G., Renieri, A., & Meloni, I. (2020). AAV-mediated FOXG1 gene editing in human Rett primary cells. *European journal of human genetics : EJHG*, 28(10), 1446–1458.
72. Croci, S., Carriero, M. L., Capitani, K., Daga, S., Donati, F., Frullanti, E., Lamacchia, V., Tita, R., Giliberti, A., Valentino, F., Benetti, E., Ciabattini, A., Furini, S., Lo Rizzo, C., Pinto, A. M., Conticello, S. G., Renieri, A., & Meloni, I. (2020). High rate of HDR in gene editing of p.(Thr158Met) MECP2 mutational hotspot. *European journal of human genetics : EJHG*, 28(9), 1231–1242.
73. Fahn S (2015) The medical treatment of Parkinson disease from James Parkinson to George Cotzias. *Mov Disord* 30, 4–18
74. Friedmann T, Roblin R (1972) Gene therapy for human genetic disease? *Science* 175, 949–955

75. S.L. Ginn, A.K. Amaya, I.E. Alexander, M. Edelstein, M.R. Abedi Gene therapy clinical trials worldwide to 2017: an update *J. Gene Med.*, 20 (5) (2018), p. e3015
76. J. Hoggatt Gene therapy for “Bubble Boy” disease *Cell*, 166 (2) (2016), p. 263
77. J. Glascock, M. Lenz, K. Hobby, J. Jarecki Cure SMA and our patient community celebrate the first approved drug for SMA *Gene Ther.*, 24 (9) (2017), pp. 498-500)
78. R. Korinthenberg A new era in the management of Duchenne Muscular Dystrophy *Dev. Med. Child Neurol.*, 61 (3) (2019), pp. 292-297
79. Moses D, Drago J, Teper Y, et al. Fetal striatum- and ventral mesencephalon-derived expanded neurospheres rescue dopaminergic neurons in vitro and the nigrostriatal system in vivo. *Neuroscience* 2008 Jun 23; 154(2): 606–20
80. Sun J, Gao Y, Yang L, et al. Neural-tube-derived neuro-epithelial stem cells: a new transplant resource for Parkinson’s disease. *Neuroreport* 2007 Apr 16; 18(6): 543–7
81. Takagi Y, Takahashi J, Saiki H, et al. Dopaminergic neurons generated from monkey embryonic stem cells function in a Parkinson primate model. *J Clin Invest* 2005 Jan; 115(1): 102–9
82. Muramatsu SI, Fujimoto KI, Ikeguchi K, Shizuma N, Kawasaki K, Ono F, Shen Y, Wang L, Mizukami H, Kume A et al (2002) Behavioral recovery in a primate model of Parkinson's disease by triple transduction of striatal cells with adeno-associated viral vectors expressing dopamine-synthesizing enzymes. *Hum Gene Ther* 13: 345–354
83. Richardson RM, Varenika V, Forsayeth JR, Bankiewicz KS. Future applications: gene therapy. *Neurosurg Clin N Am.* 2009;20:205–210

84. Palfi S, Gurruchaga JM, Lepetit H, Howard K, Ralph GS, Mason S, Gouello G, Domenech P, Buttery PC, Hantraye P, Tuckwell NJ, Barker RA, Mitrophanous KA (2018) Long-term follow-up of a Phase I/II study of ProSavin, a lentiviral vector gene therapy for Parkinson's disease. *Hum Gene Ther Clin Dev* 29, 148–155
85. Khalil A.M. The genome editing revolution. *J. Genet. Eng. Biotechnol.* 2020;18:68
86. Chen Y., Dolt K.S., Kriek M., Baker T., Downey P., Drummond N.J., Canham M.A., Natalwala A., Rosser S., Kunath T. Engineering synucleinopathy-resistant human dopaminergic neurons by CRISPR-mediated deletion of the SNCA gene. *Eur. J. Neurosci.* 2019;49:510–524.
87. Komor A. C., Kim Y. B., Packer M. S., Zuris J. A., Liu D. R. Programmable editing of a target base in genomic DNA without double-stranded DNA cleavage. *Nature.* 2016;533(7603):420–424.
88. Gaudelli, N. M., Komor, A. C., Rees, H. A., Packer, M. S., Badran, A. H., Bryson, D. I., & Liu, D. R. (2017). Programmable base editing of A•T to G•C in genomic DNA without DNA cleavage. *Nature*, 551(7681), 464–471.
89. Gaudelli, N. M., Lam, D. K., Rees, H. A., Solá-Esteves, N. M., Barrera, L. A., Born, D. A., Edwards, A., Gehrke, J. M., Lee, S. J., Liquori, A. J., Murray, R., Packer, M. S., Rinaldi, C., Slaymaker, I. M., Yen, J., Young, L. E., & Ciaramella, G. (2020). Directed evolution of adenine base editors with increased activity and therapeutic application. *Nature biotechnology*, 38(7), 892–900.
90. Song, C. Q., Jiang, T., Richter, M., Rhym, L. H., Koblan, L. W., Zafra, M. P., Schatoff, E. M., Doman, J. L., Cao, Y., Dow, L. E., Zhu, L. J., Anderson, D.

- G., Liu, D. R., Yin, H., & Xue, W. (2020). Adenine base editing in an adult mouse model of tyrosinaemia. *Nature biomedical engineering*, 4(1), 125–130.
91. Zeng, Y et al. Correction of the marfan syndrome pathogenic FBN1 mutation by base editing in human cells and heterozygous embryos. *Mol. Ther.* 26, 2631–2637 (2018)
 92. Song, C.-Q. et al. Adenine base editing in an adult mouse model of tyrosinaemia. *Nat. Biomed. Eng.* 4, 125–130
 93. Zhang, X., Zhu, B., Chen, L. et al. Dual base editor catalyzes both cytosine and adenine base conversions in human cells. *Nat Biotechnol* 38, 856–860 (2020).
 94. Newby, G. A., Yen, J. S., Woodard, K. J., Mayuranathan, T., Lazzarotto, C. R., Li, Y., Sheppard-Tillman, H., Porter, S. N., Yao, Y., Mayberry, K., Everette, K. A., Jang, Y., Podracky, C. J., Thaman, E., Lechauve, C., Sharma, A., Henderson, J. M., Richter, M. F., Zhao, K. T., Miller, S. M., ... Liu, D. R. (2021). Base editing of haematopoietic stem cells rescues sickle cell disease in mice. *Nature*, 595(7866), 295–302.
 95. Koblan, L. W., Erdos, M. R., Wilson, C., Cabral, W. A., Levy, J. M., Xiong, Z. M., Tavaréz, U. L., Davison, L. M., Gete, Y. G., Mao, X., Newby, G. A., Doherty, S. P., Narisu, N., Sheng, Q., Krilow, C., Lin, C. Y., Gordon, L. B., Cao, K., Collins, F. S., Brown, J. D., ... Liu, D. R. (2021). In vivo base editing rescues Hutchinson-Gilford progeria syndrome in mice. *Nature*, 589(7843), 608–614.
 96. Sipe, C. J., Kluesner, M. G., Bingea, S. P., Lahr, W. S., Andrew, A. A., Wang, M., DeFeo, A. P., Hinkel, T. L., Laoharawee, K., Wagner, J. E., MacMillan, M. L., Vercellotti, G. M., Tolar, J., Osborn, M. J., McIvor, R. S., Webber, B. R., & Moriarity, B. S. (2022). Correction of Fanconi Anemia Mutations Using Digital

- Genome Engineering. *International journal of molecular sciences*, 23(15), 8416.
97. Swiech, L., Heidenreich, M., Banerjee, A., Habib, N., Li, Y., Trombetta, J., ... & Zhang, F. (2015). In vivo interrogation of gene function in the mammalian brain using CRISPR- Cas9. *Nat Biotechnol*, 33(1), 102-106
 98. Dracopoli, N. C., Haines, J. L., & Korf, B. R. (1994). *Current protocols in human genetics*
 99. Park, J., Lim, K., Kim, J. S., & Bae, S. (2017). Cas-analyzer: an online tool for assessing genome editing results using NGS data. *Bioinformatic*
 100. Hwang, GH., Park, J., Lim, K. et al. Web-based design and analysis tools for CRISPR base editing. *BMC Bioinformatics* 19, 542 (2018).
 101. Manghwar, H., Lindsey, K., Zhang, X., & Jin, S. (2019). CRISPR/Cas System: Recent Advances and Future Prospects for Genome Editing. *Trends in plant science*, 24(12), 1102–1125.
 102. Qin JY, Zhang L, Clift KL, Huler I, Xiang AP, Ren B-Z, et al. (2010) Systematic Comparison of Constitutive Promoters and the Doxycycline-Inducible Promoter. *PLoS ONE* 5(5): e10611
 103. Marsden C. D. (1994). Problems with long-term levodopa therapy for Parkinson's disease. *Clinical neuropharmacology*, 17 Suppl 2, S32–S44
 104. Malek N. (2019). Deep Brain Stimulation in Parkinson's Disease. *Neurology India*, 67(4), 968–978.
 105. Tolosa, E., Vila, M., Klein, C., & Rascol, O. (2020). LRRK2 in Parkinson disease: challenges of clinical trials. *Nature reviews. Neurology*, 16(2), 97–107.
 106. Jennings, D., Huntwork-Rodriguez, S., Henry, A. G., Sasaki, J. C., Meisner, R., Diaz, D., Solanoy, H., Wang, X., Negrou, E., Bondar, V. V., Ghosh, R.,

- Maloney, M. T., Propson, N. E., Zhu, Y., Maciuca, R. D., Harris, L., Kay, A., LeWitt, P., King, T. A., Kern, D., ... Troyer, M. D. (2022). Preclinical and clinical evaluation of the LRRK2 inhibitor DNL201 for Parkinson's disease. *Science translational medicine*, 14(648), eabj2658.
107. Taymans JM, Greggio E. LRRK2 Kinase Inhibition as a Therapeutic Strategy for Parkinson's Disease, Where Do We Stand? *Curr Neuropharmacol*. 2016;14(3):214-25.
108. De Wit, T., Baekelandt, V., & Lobbstaël, E. (2018). LRRK2 Phosphorylation: Behind the Scenes. *The Neuroscientist : a review journal bringing neurobiology, neurology and psychiatry*, 24(5), 486–500.
109. Martufi, M., Good, R. B., Rapiteanu, R., Schmidt, T., Patili, E., Tvermosegaard, K., New, M., Nanthakumar, C. B., Betts, J., Blanchard, A. D., & Maratou, K. (2019). Single-Step, High-Efficiency CRISPR-Cas9 Genome Editing in Primary Human Disease-Derived Fibroblasts. *The CRISPR journal*, 2(1), 31–40.
110. Herzig, M. C., Kolly, C., Persohn, E., Theil, D., Schweizer, T., Hafner, T., Stemmelen, C., Troxler, T. J., Schmid, P., Danner, S., Schnell, C. R., Mueller, M., Kinzel, B., Grevot, A., Bolognani, F., Stirn, M., Kuhn, R. R., Kaupmann, K., van der Putten, P. H., Rovelli, G., ... Shimshek, D. R. (2011). LRRK2 protein levels are determined by kinase function and are crucial for kidney and lung homeostasis in mice. *Human molecular genetics*, 20(21), 4209–4223.
111. Ran, F. A., Cong, L., Yan, W. X., Scott, D. A., Gootenberg, J. S., Kriz, A. J., Zetsche, B., Shalem, O., Wu, X., Makarova, K. S., Koonin, E. V., Sharp, P. A., & Zhang, F. (2015). In vivo genome editing using *Staphylococcus aureus* Cas9. *Nature*, 520(7546), 186–191.

112. Megumi Adachi, Edward W. Keefer, Frederick S. Jones, A segment of the Mesp2 promoter is sufficient to drive expression in neurons, *Human Molecular Genetics*, Volume 14, Issue 23, 1 December 2005, Pages 3709–3722
113. Qin JY, Zhang L, Clift KL, Huler I, Xiang AP, Ren B-Z, et al. (2010) Systematic Comparison of Constitutive Promoters and the Doxycycline-Inducible Promoter. *PLoS ONE* 5(5): e10611)
114. Zhong, Z., Sretenovic, S., Ren, Q., Yang, L., Bao, Y., Qi, C., Yuan, M., He, Y., Liu, S., Liu, X., Wang, J., Huang, L., Wang, Y., Baby, D., Wang, D., Zhang, T., Qi, Y., & Zhang, Y. (2019). Improving Plant Genome Editing with High-Fidelity xCas9 and Non-canonical PAM-Targeting Cas9-NG. *Molecular plant*, 12(7), 1027–1036.
115. Chang, K. H., Huang, C. Y., Ou-Yang, C. H., Ho, C. H., Lin, H. Y., Hsu, C. L., Chen, Y. T., Chou, Y. C., Chen, Y. J., Chen, Y., Lin, J. L., Wang, J. K., Lin, P. W., Lin, Y. R., Lin, M. H., Tseng, C. K., & Lin, C. H. (2021). In vitro genome editing rescues parkinsonism phenotypes in induced pluripotent stem cell-derived dopaminergic neurons carrying LRRK2 p.G2019S mutation. *Stem cell research & therapy*, 12(1), 508

7. List of Abbreviations

PD = Parkinson Disease

LB = Lewy bodies

BBB =Blood Brain Barrier

CNS = Central Nervous system

DBS = Deep brain stimulation

CRISPR = Clustered regularly interspaced short palindromic repeats

Cas9 = CRISPR associated enzyme

PAM = Protospacer adjacent motif

DSB = Double strand break

NHEJ = Non Homologous End Joining

BE = Base Editor

ABE = Adenine Base Editor

CBE = Cytosine Base Editor

HEK = human embryonic kidney

CMV = Citomegalovirus

MECP2 = Methyl-CpG- binding protein 2

EF1a = elongation factor 1 alpha